THE JOURNAL OF COMPARATIVE NEUROLOGY 335:437–459 (1993)

Tonotopic Organization, Architectonic Fields, and Connections of Auditory Cortex in Macaque Monkeys

A. MOREL, P.E. GARRAGHTY, AND J.H. KAAS
Department of Psychology, Vanderbilt University, Nashville, Tennessee 37240

ABSTRACT

Microelectrode recordings were used to investigate the tonotopic organization of auditory cortex of macaque monkeys and guide the placement of injections of wheat germ agglutinin-horse radish peroxidase (WGA-HRP) and fluorescent dyes. Anatomical and physiological results were later related to histological distinctions in the same brains after sections were processed for cytoarchitecture, myeloarchitecture, acetylcholinesterase (AchE), or cytochrome oxidase (CO). The experiments produced several major findings. (1) Neurons throughout a broad expanse of cortex were highly responsive to pure tones, and best frequencies could be determined for neurons in arrays of recording sites. (2) The microelectrode recordings revealed two systematic representations of tone frequencies, the primary area (AI) and a primary-like rostral field (R) as previously described. The representation of high to low frequency tones in A1 was largely caudorostral along the plane of the sulcus. A reversal of the order of representation of frequencies occurred in R. (3) AI and R together were coextensive with a koniocellular, densely myelinated zone that expressed high levels of AchE and CO. These architectonic features were somewhat less pronounced in R than AI, but a clear border between the two areas was not apparent. (4) Cortex bordering AI and R was less responsive to tones, but when best frequencies for neurons could be determined, they matched those for adjoining parts of AI and R. (5) Architectonically distinct regions were apparent within some of the cortex bordering AI and R. (6) The major ipsilateral cortical connections of AI were with R and cortex immediately lateral and medial to AI. (7) Callosal connections of AI were predominately with matched locations in the opposite AI, but they also included adjoining fields. (8) Neurons in the ventral (MG_V), medial (MG_M), and dorsal (MG_D) nuclei of the medial geniculate complex projected to AI and cortex lateral to AI. (9) Injections in cortex responsive to high frequency tones labeled more dorsal parts of MG_V than injections in cortex responsive to low frequency tones.

Key words: medial geniculate complex, corpus callosum, thalamus, sensory systems, primates

The nervous system of macaque monkeys has been studied extensively because of the widespread and supportable belief that the brains of these primates more closely resemble those of humans than do the brains of other commonly available experimental mammals. In particular, over the last twenty years we have greatly increased our understanding of the organization and connections of the visual system in macaques, where over thirty visual areas and hundreds of connections have been proposed (for review, see Felleman and Van Essen, '91). Considerable progress has also been made in studying the somatosensory system, where the significance of the traditional architectonic subdivisions of anterior parietal cortex as four representations of body receptors is now understood, subdivisions of lateral and insular somatosensory cortex have been proposed, and connection patterns of most of these fields have been described (for review, see Kaas and Pons, '88). In contrast, relatively little progress has been made in understanding the organization of the auditory system in macaque monkeys. While microelectrode mapping approaches in combination with studies of architectonics and patterns of connections have been used repeatedly to investigate the organization of the visual and somatosensory cortex and thalamus, there is only a single microelectrode mapping

Accepted May 6, 1993.

Dr. Morel's present address is Laboratory for Functional Neurosurgery, Neurosurgery Clinic, 100 Rämistrasse, University Hospital, CH-8091 Zürich, Switzerland.

Dr. Garraghty's present address is Department of Psychology, Indiana University, Bloomington, IN 47405.

Address reprint requests to Jon H. Kaas, Department of Psychology, 301 Wilson Hall, Vanderbilt University, Nashville, TN 37240.

study of auditory cortex in macaques, and that landmark study (Merzenich and Brugge, '73) has not been followed by others in nearly 20 years. The several important studies of the connections of cortex in the auditory region (e.g., Walker, '37; Mesulam and Pandya, '73; Burton and Jones, '76; Galaburda and Pandya, '83) relied on relating connection and architectonic patterns, and did not use electrophysiological data to define fields or locate injection sites. However, such combined approaches have been used effectively in studies of auditory cortex in New World monkeys (FitzPatrick and Imig, '78, '80; Aitkin et al., '88; Luethke et al., '89; Morel and Kaas, '92), cats (e.g., Imig and Reale, '80; Andersen et al., '80; Imig and Morel, '83; Clarey and Irvine, '90); and squirrels (Luethke et al., '88). Further studies on macaques are needed because models of cortical organization derived from cats may have limited usefulness in understanding primates, and it is uncertain how extensively models of organization based on New World monkeys apply to other primate taxa including macaques and humans. Thus, the broad goal of the present study was to start to investigate the organization of auditory cortex in macaques using the combined methods that have been so useful in studies of the visual and somatosensory systems, and the auditory cortex of other mammals.

In this investigation, we reconsidered the issue of how auditory cortex is tonotopically organized in the region of the primary field (AI) and the primary-like rostral field (R) (or rostrolateral, RL[1]) of Merzenich and Brugge ('73). We subsequently related the physiological results to cytoarchitectonic and myeloarchitectonic patterns, as well as differences in expressed levels of cytochrome oxidase (CO) and acetylcholinesterase (AchE) in the same animals. Finally, we determined cortical and thalamic connection patterns by placing injections of tracers at physiologically identified sites along and within AI.

Our approach was designed to address several questions about the organization and connections of auditory cortex in macaques. First, we hoped to complement and extend the early microelectrode mapping experiments of Merzenich and Brugge ('73) by obtaining recordings from additional monkeys and possibly from cortex not fully explored in those initial studies. Second, we planned to describe more fully the architectonic features of physiologically defined subdivisions of auditory cortex by including procedures for revealing CO and AchE levels and myelin stains, since these procedures have been used to effectively reveal subdivisions of cortex elsewhere (e.g., Bear et al., '85; Tootell et al., '85; Luethke et al., '89; Wallace et al., '91; Morel and Kaas, '92). Third, we sought to determine the connections of auditory cortex by placing injections in and just lateral to AI. By placing injections of different tracers in sites responsive to different frequencies in the same monkeys, we obtained evidence from connection patterns on the tonotopic organization of nuclei in the medial geniculate complex of macaques. Some of these results have been briefly presented elsewhere (Morel et al., '91).

MATERIALS AND METHODS

The surgical preparation, acoustical stimulation, and recording procedures were similar to those described previously (Luethke et al., '89; Morel and Kaas, '92). Adult macaque monkeys (*Macaca fascicularis*) were selected by otoscopic examination for unobstructed external auditory meatus. Each monkey was premedicated with dexamethasone (1 mg/kg) and then anesthetized with ketamine hydrochloride (20–30 mg/kg) supplemented by xylazine (2 mg/kg). Additional doses of anesthetic (5–10 mg/kg) were given periodically during surgery and recordings to maintain a surgical level of anesthesia. Surgery was performed under aseptic conditions. The body temperature was maintained around 38°C with a heating pad, and the electrocardiogram was also monitored. After retraction of the temporal muscle, a craniotomy was used to expose the superior temporal gyrus and overlying part of the parietofrontal cortex; the dura was retracted, and the cortex covered with silicone oil to prevent desiccation. Photographs of the cortical surface were enlarged for later use in marking the positions of electrode penetrations in relation to blood vessels and the sulcal pattern.

Acoustical stimulation and recordings

During recording, the animal's head was held firmly in a stereotaxic position with a bar cemented on the occiput and attached to the stereotaxic frame, leaving free access to the ears. Auditory stimulation consisted of pure tones of varying frequencies and intensities produced by a Krohn-Hite oscillator and shaped into 100–200 msec pulses with an electronic switch. The intensity of the tone bursts was preadjusted with an EXP-1 amplifier, and the stimuli delivered to the contralateral ear via a flexible hollow ear tube coupled to an audiometric driver that has been previously calibrated (see Morel and Kaas, '92). Other acoustic stimuli, such as clicks or speech sounds were also presented during recording.

Multi-unit activity was recorded with low impedance (1–1.5 M ohms) microelectrodes advanced with a hydraulic micromanipulator. The signal from the electrode was amplified, filtered, displayed on an oscilloscope and monitored through a loudspeaker. Small electrolytic lesions were made along penetrations to mark physiologically identified locations to later aid in histological reconstructions of positions of recording sites. As in previous studies (Luethke et al., '89; Morel and Kaas, '92), best frequencies were determined audiovisually by decreasing tone intensity and thereby decreasing the range of frequencies producing a noticeable response. The best frequency was the frequency where the lowest intensity produced a noticeable response. Responses to tones and best frequencies for neurons or clusters of neurons were recorded at 0.1–0.3 mm intervals along each electrode penetration. Lateromedial electrode penetrations were oriented 10° to 30° from the horizontal plane to be parallel to the cortex of the ventral bank of the lateral sulcus. Because of the irregularity of the surface of the cortex along the lower bank of the lateral sulcus, the electrode angle was occasionally changed during the course of an experiment, especially when moving from posterior to anterior along the sulcus. Electrode penetrations were placed about 1 mm apart.

Tracer injections

After 5–7 hours of recording, 1 to 3 different tracers were placed in locations in auditory cortex defined by recordings. The tracers were horseradish peroxidase conjugated to wheat germ agglutinin (WGA-HRP, 1% in saline), and fluorescent dyes [3% fast blue (FB) or diamidino-yellow

[1]Merzenich and Brugge ('73) termed the field RL for rostralateral, but the term R for rostral is used here because the term R was subsequently used in other studies (Imig et al., '77; FitzPatrick and Imig, '80; Morel and Kaas, '92).

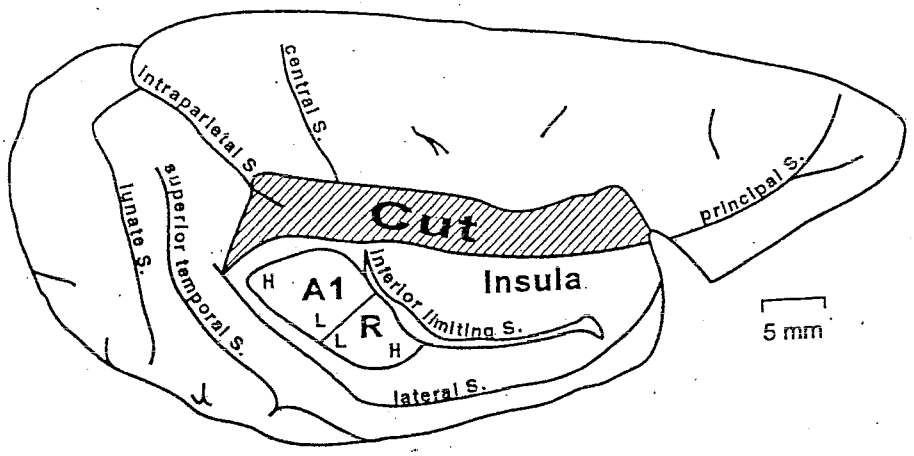

Fig. 1. The locations of AI and R on the lower bank of the lateral sulcus. In this dorsal view of the right hemisphere of a macaque brain, lateral portions of parietal and frontal cortex have been removed (cut) to expose cortex on the lower bank of the lateral sulcus (the superior temporal plane) and the insula. AI and R have mirror-reverse tonotopic organizations from high (H) to low (L). AI, primary auditory cortex; R, the rostral auditory area; inferior lim. S., inferior limiting sulcus.

(DY) in saline]. The injections were made with a glass micropipette sealed to the needle of a 1 or 5 μl Hamilton microsyringe. The total amount injected varied between 0.05 μl (for WGA-HRP) and 1 μl (for fluorescent dyes). Following injections, the skull opening was closed with dental acrylic over the bone flap, and the skin sutured. The animals were carefully monitored during recovery from anesthesia, and allowed to survive 3 to 15 days depending on the tracer or tracers used.

Histological procedures

At the end of the survival period, the animals were reoperated and auditory cortex contralateral to the injected hemisphere was mapped extensively. Following the recording session, a lethal dose of pentobarbital was given, and the animals were perfused through the heart with saline followed by 4% (for HRP) or 6% (for fluorescent dyes) paraformaldehyde in phosphate buffer and, successively, 20% and 30% sucrose solutions in the same buffer. After perfusion, the brains were immediately removed, photographed, and separated into two blocks by a frontal section just caudal to the arcuate sulcus. The blocks were soaked for a few hours in 30% sucrose in phosphate buffer, then cut at 40 μm in the coronal plane on a freezing microtome. Alternate series of sections were mounted for fluorescent microscopy, processed for HRP following a low artifact TMB procedure (Gibson et al., '84), stained for Nissl with cresyl violet, stained for myelin with the Gallyas ('79) method, processed for cytochrome oxidase (CO; Wong-Riley, '79), or processed for acetylcholinesterase (AChE; Geneser-Jensen and Blackstad, '71).

Data analysis

Sections containing fluorescent label were observed and plotted under ultraviolet (UV) illumination with a Leitz microscope equipped with a computer-assisted X-Y plotting system (Bioquant System, R & M Biometrics, Inc.). Detailed enlarged drawings of sections containing electrode tracks, architectonic boundaries, injection sites, and label distributions were used for three-dimensional reconstructions of the auditory cortex. These were obtained by tracing the contours of individual sections spaced approximately 200 μm apart, on enlarged photographs of the brain surface. Part of the upper bank of the lateral sulcus was removed in the illustrations, and cortex was partly unfolded to expose the surface of the supratemporal plane.

RESULTS

In the present study, we investigated the tonotopic organization, architecture, and connections of auditory cortex in macaque monkeys. The physiological results are presented first. They provide evidence for two primary-like fields, AI and R, as previously reported by Merzenich and Brugge ('73). Next, we describe the architectonic characteristics of AI, R, and surrounding cortex. Finally, the cortical and thalamic connections of AI are described.

Neuron response characteristics and tonotopic patterns

Recordings were obtained from neurons along the superior temporal plane of macaque monkeys by angling mediolateral electrode penetrations in a nearly horizontal plane from the outer ventral lip to the fundus of the lateral sulcus or the inferior outer bank of the inferior limiting sulcus. By adjusting the angle and placement of such penetrations, we were able to record from neurons in the middle layers of cortex over long sequences. Typically we were able to elicit clear responses to tones and other auditory stimuli at numerous sites along the extents of the electrode penetrations. Neurons in one large region responded vigorously to narrow ranges of pure tones with short response latencies, and threshold responses at specific frequencies could be determined. This large region is outlined on the surface of the lower bank of the lateral sulcus in Figure 1 as AI plus R.

Recordings from AI and R were obtained both during brief sessions as a guide to locating favorable sites for the injection of tracers and later in the opposite hemisphere in long sessions just before sacrifice. Results from the longer recording sessions in four monkeys are summarized in Figures 2 and 3. In each case, cortex in the region of AI and

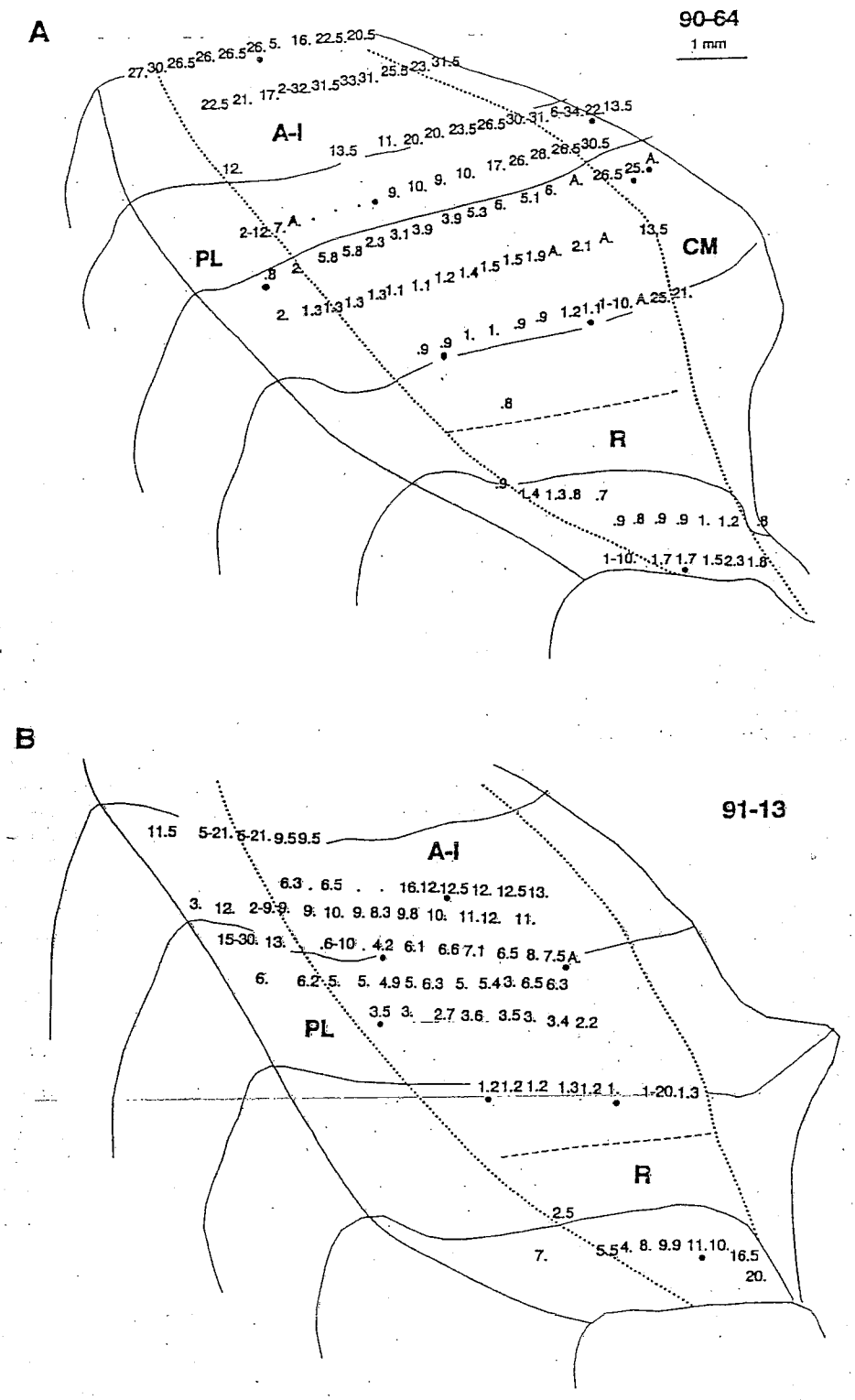

Fig. 2. Best frequencies for neurons at recording sites in auditory cortex of monkey 90-64 (A) and 91-13 (B). Each figure is a reconstructed frontal-dorsolateral view of cortex of the superior temporal plane of the lateral sulcus. Some of the lines of individual coronal brain sections are preserved, and areas AI and R, as determined architectonically, are outlined (dotted lines). A dashed line marks the estimated border of AI with R. Electrodes penetrated cortex lateromedially. Recording sites along those penetrations are projected on to the surface and marked with small dots. Numbers next to dots indicate the best frequencies in kH_Z for neurons recorded at each site. Thus, neurons in the caudal row of sites in A had best frequencies in the 16–30 kH_Z range, while the most rostrolateral sites in AI had best frequencies of less than 1 kH_Z. At some locations, a best frequency was not determined, but a range of effective frequencies was recorded and indicated in the figure (e.g., 5-21). Large dots mark locations of microlesions used to help relate recordings to architectonic results. Auditory sites that responded poorly to tones are marked with A. AI, primary auditory cortex; R, the rostral auditory area; PL, the posterior lateral field; CM, the caudomedial field.

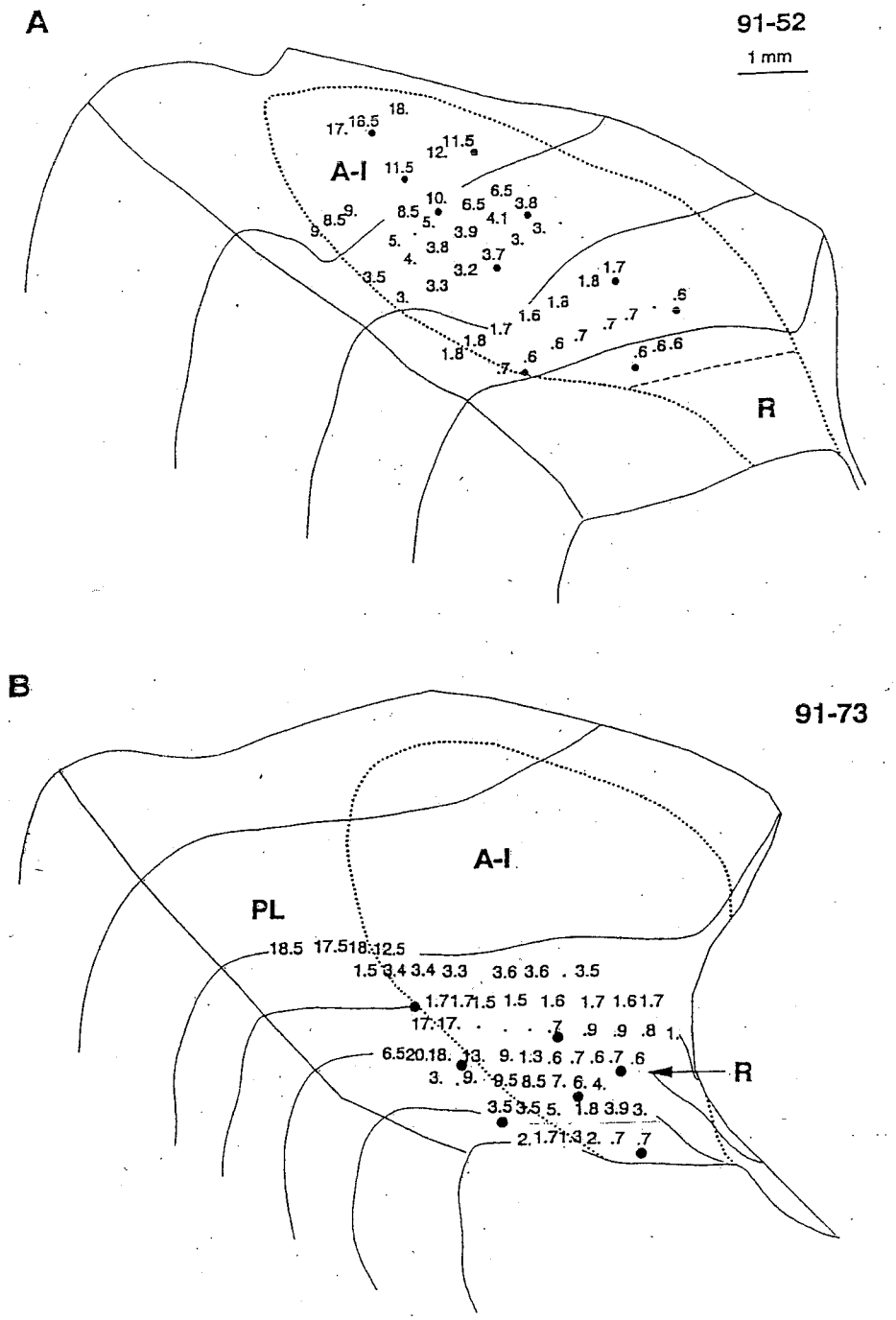

Fig. 3. Best frequencies for neurons at designated recording sites in cases 91-52 (A) and 91-73 (B). Other conventions as in Figure 2. In B, an arrow marks the approximate level of a transition to R.

R was reconstructed from serial coronal brain sections so that the cortex of superior temporal plane could be shown as a three-dimensional surface from a frontolateral perspective with recording sites and architectonic boundaries projected onto the surface. Most recordings were from clusters of neurons rather than single neurons, but neurons recorded at each site had similar best frequencies, and thus we best realized our goal of sampling many sites by not attempting to isolate single neurons. Best frequencies ranged from over 30 kH_Z to less than 1 kH_Z. Sometimes, the neurons responded poorly to tones, or the tuning curve was broad, so that a best frequency was not determined, and only a range of effective frequencies was determined. Neurons at other sites responded to clicks and other auditory stimuli, but responded poorly to tones. When the locations of recording sites were related to the types of

responses, the unresponsive, poorly responsive, and broadly tuned neurons tended to be outside of AI and R, or above or below the middle layers (IV and III) of cortex.

AI and R. The recording results support the conclusion of Merzenich and Brugge ('73) that auditory cortex includes two tonotopically organized fields, AI and R, that are both primary-like in responsiveness to tones. Most of our recordings were from AI, but enough recordings were obtained from R to provide evidence for this second field.

Our most extensive map was obtained from case 90-64 (Fig. 2A), and this map revealed the basic tonotopic organization of AI and provided evidence for R. We see from this case that high frequency tones were represented caudomedially and low frequency tones rostralaterally in AI. Lines of isofrequency were in a lateromedial plane in caudal AI, but they tended to curve rostrally in rostromedial AI. Thus, neurons in the most caudal recording sites in AI in case 90-64 were best activated by tones in the 20–30 kH_Z range, and neurons across the complete width of caudal AI were best activated by high frequencies. More rostrally, neurons near the lateral border of AI were activated by midfrequency tones, but deeper recording sites revealed neurons most responsive to high frequencies. In the most rostrolateral portion of AI, neurons responded best to low frequencies, including frequencies of less than 1 kH_Z. However, neurons at sites deep in the sulcus, near the border of AI with CM, were activated by higher best frequencies. While a broad zone of even more rostral cortex responded to low tones, the most rostral sites in this case had neurons best activated by tones higher than 1 kH_Z. Thus, there was a return to slightly higher best frequencies for the most rostral sites in the explored region, indicating a reversal of the tonotopic progression, and providing evidence for a second area, R. The mapping results were not detailed enough to provide a precise indication of the line of reversal, but the border between AI and R is likely to be near the site with the low best frequency of 0.8 kH_Z. Most of the sites where best frequencies were determined were later found to be within the architectonic boundaries of AI and R, but some of these sites were on or outside the border. Often, neurons or clusters of neurons at these sites were less responsive to tones, and had broader tuning, but sometimes responses were not notably different from those in AI or R.

Similar results were obtained in other cases. In case 91-13 (Fig. 2B), for example, less of AI was mapped, but the same progression from the representation of higher to lower frequencies was apparent along the caudorostral extent of AI. In addition, a portion of rostromedial R responded to high frequencies of up to 20 kH_Z. Case 91-52 (Fig. 3A) provided mapping data across most of AI, including high, middle and low frequency portions, and case 91-73 (Fig. 3B) included recordings from the low frequency portion of AI and probably the adjoining low frequency portion of R. Case 90-76 (not shown) involved recordings largely in R, where much of the explored portion of the field was responsive to low frequencies. However, sites in the most rostromedial part of R on the bank of the inferior limiting sulcus responded to high frequency tones with best frequencies extending as high as 32 kH_Z. Thus, R appears to represent the frequency range as extensively as AI.

Cortex lateral and medial to AI and R. Our recordings from cortex surrounding AI and R were limited to sites lateral and medial to AI and R in penetrations passing through AI and R. In general, neurons in these regions were less responsive to tones, and responses occurred over broader frequency ranges so that best frequencies were more difficult to determine. Nevertheless, many neurons medial or lateral to AI and R were responsive to tones and other sounds, and best frequencies were sometimes determined. The results indicate that at least some of the cortex surrounding AI and R is auditory. The results also suggest that some or all of the surrounding fields have at least crude tonotopic organizations that are tonotopically matched or congruent along common borders with the representations in AI and R. Thus, electrode penetrations lateral to AI in case 91-13 (Fig. 2B), encountered neurons that responded best to higher frequencies caudally and lower frequencies rostrally in a progression that matched that in the adjoining part of AI. Similar results from this posterior lateral region, PL, were obtained in case 91-73 (Fig. 3B), and more limited recordings were made in cases 90-64 (Fig. 2A) and 91-52 (Fig. 3A). In addition, a few recordings from cortex lateral to R (case 91-73, Fig. 3B; case 91-52, Fig. 3A; case 90-64, Fig. 2A) suggested the existence of an anterior lateral field, AL, with a tonotopic organization in parallel with that in R. Finally, recordings medial to AI, largely obtained in case 90-64 (Fig. 2A), revealed responsiveness to high frequency tones near AI with a suggestion of a progression toward low frequency tones away from AI. We refer to this region as the caudomedial field, CM, after Merzenich and Brugge, ('73).

Architectonic subdivisions of auditory cortex

We examined the regions of auditory cortex explored during recording sessions for architectonic features that would usefully identify auditory fields. Sections from the experimental brains were stained with cresyl violet to reveal cell bodies, stained for myelinated fibers, or processed for levels of CO or AchE. Architectonic features of this region of cortex were then related to the physiological results from the same animal. The major findings were that AI and R resemble each other architectonically, and that these two fields are quite distinct from surrounding cortex. In addition, cortex surrounding AI and R can be subdivided on the basis of architectonic differences. In this section, we first describe AI and R, relate some of the physiological results that indicate that a large architectonic field is coextensive with AI and R, and then describe several subdivisions of surrounding cortex.

AI and R. The region we have electrophysiologically defined as AI plus R is architectonically distinct from surrounding cortex. In brain sections stained with cresyl violet, AI is easily identified by a broad layer IV that is densely packed with small granule cells, densely packed cells in inner layer III, and a rather dark and dense layer VI (Fig. 4c and f; also see Merzenich and Brugge, '73). These are well-known cytoarchitectonic features of primary sensory fields, which are sometimes referred to as koniocortical fields because of the small densely packed granule cells (see von Bonin and Bailey, '47). In sections processed for CO, layer IV and inner layer III of AI stain quite darkly, and there is a marked reduction in the amount of CO expressed in these layers in surrounding cortex (Fig. 4b and e). We have also examined auditory cortex in brain sections from monkeys used in studies of patterns of metabolic activity in the brain with the radioactive 2-deoxyglucose (2-DG) method, and found that high levels of deoxyglucose are incorporated in the middle layers of AI, even during periods of quiet. Cortex in the expected location of AI was also densely labeled with 2-deoxyglucose in the study of somatosensory cortex of the lateral sulcus by Juliano et al. ('83). AI

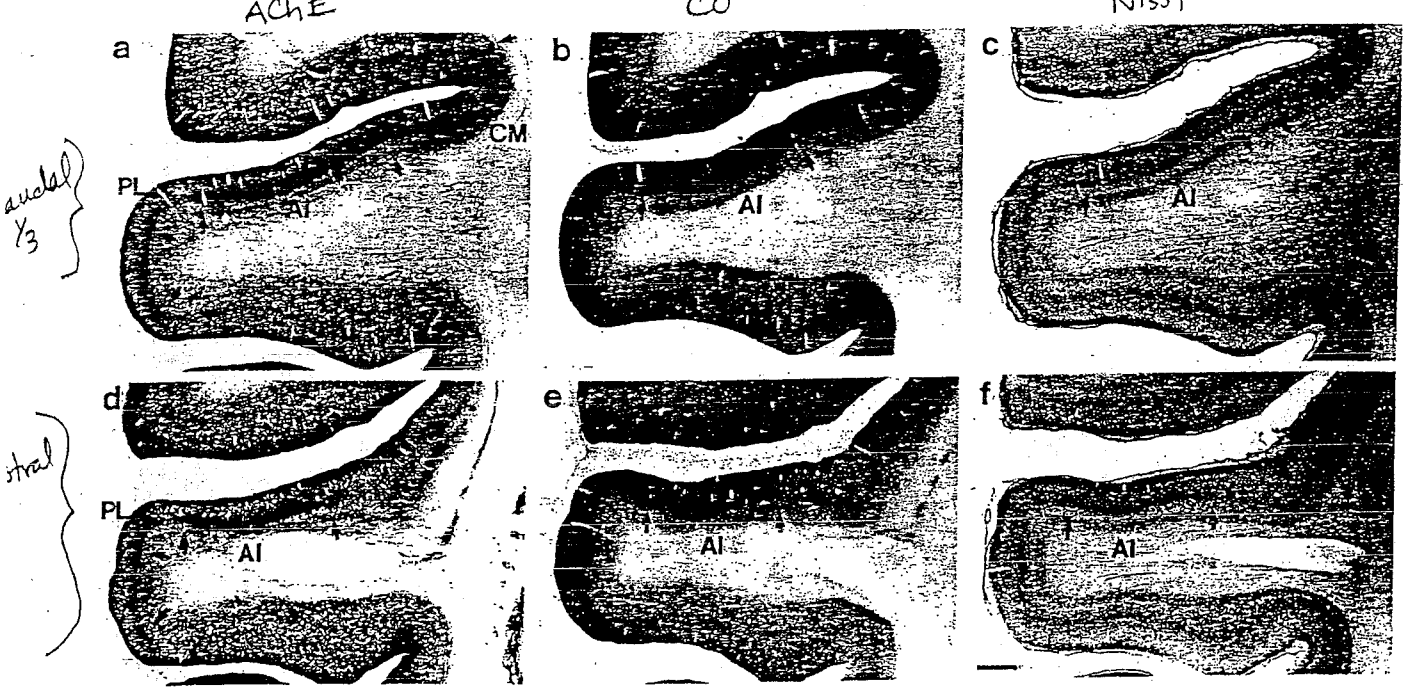

Fig. 4. The architecture of AI and surrounding cortex. **a–c** are adjacent coronal sections through the caudal third of AI; **d–f** are through the rostral third of AI. Sections a and d were processed for acetylcholinesterase (AchE), b and e for cytochrome oxidase (CO), and c and f for Nissl substance. Arrows mark the borders of AI. The estimated extent of the caudomedial area (CM) is indicated in a. Other arrows in a and d mark the lateral limit of PL and an area extending ventrally to the lip of the superior temporal sulcus. Scale bar = 1 mm and applies to a–f.

is also quite obvious in sections stained for AchE, since the expression of AchE in layer IV is exceedingly dense in AI, compared to surrounding areas (Fig. 4a and d). AI is also marked by dense myelination (Fig. 6). The inner and outer bands of Baillarger are well developed, with the inner band being particularly dense (also see Pandya and Sanides, '73).

Area R has architectonic features that are very similar, though somewhat less pronounced, to those of AI (Fig. 5). Thus, R has the koniocellular characteristic of a broad layer IV that is densely packed with small cells, a higher level of CO and AchE expression in layer IV, and dense bands of myelin. Merzenich and Brugge ('73) also noted that R (their RL) resembles AI in cytoarchitecture, but concluded that the packing of small cells was less dense in R. Our coronal plane of section did not optimize comparisons of A-I and R at the border, and we are uncertain if the transition from one field to the other can be reliably detected.

A correspondence of AI to auditory koniocortex was demonstrated by relating physiological to architectonic results by using marking microlesions to identify electrode penetrations and recording sites in stained brain sections. An example of this approach is shown in Figure 7, where each of three adjacent brain sections along an electrode tract were processed for different architectonic features. In each section, three microlesions are apparent. The lateral and medial lesions (marked L_1 and L_2 in the middle panel) were placed along one horizontal penetration and the best frequencies for neurons at recording sites along the penetration are indicated just under the track. The first lesion was placed where the neurons first responded vigorously to tones and where a clear best frequency was obtained. Neurons at subsequent recording sites were very responsive to tones (except for the sites marked A, where responses to tones were poor). The second lesion was placed at the end of a sequence of four sites where neurons were difficult to characterize or responded to high frequencies. Note that the lesion on the left was on the outer border of AI, whether defined by AchE (Fig. 7a), CO (Fig. 7b), or cytoarchitecture (Fig. 7c). However, the deep lesion on the right was about 0.5 mm deeper than the border of AI. Thus, the sequence of recording sites with neurons having best frequencies in the low to middle frequency range covered the full extent of AI, while three sites at the end of the penetration with neurons with best frequencies in the high frequency range were on the border or outside of AI.

The results of a sequence of recording sites across R are shown in Figure 8. As in Figure 7, three adjacent sections were processed for AchE (Fig. 8a), CO (Fig. 8b), or cytoarchitecture (Fig. 8c). A microlesion placed at the end of a horizontal microelectrode penetration is apparent in each section and the best frequencies for neurons recorded at sites along the penetration are indicated in Figure 8. Because R curves ventrally on the caudal bank of the inferior limiting sulcus, the penetration did not pass from border to border in R. Nevertheless, it is apparent that recording sites across most of the width of R at this level responded best to low frequencies, and there was a tendency toward higher best frequencies as sites deeper in the penetration were encountered. Such results indicate that sites throughout auditory koniocortex have neurons that respond well to tones and have best frequencies that relate to systematic patterns of frequency shift.

Fields bordering AI and R. Cortex surrounding AI and R did not have the general features of primary sensory cortex in that less CO and AchE were expressed and the middle layers of cortex were less packed with small cells. However, this surrounding cortex was not uniform in appearance, and we distinguished several regions as pre-

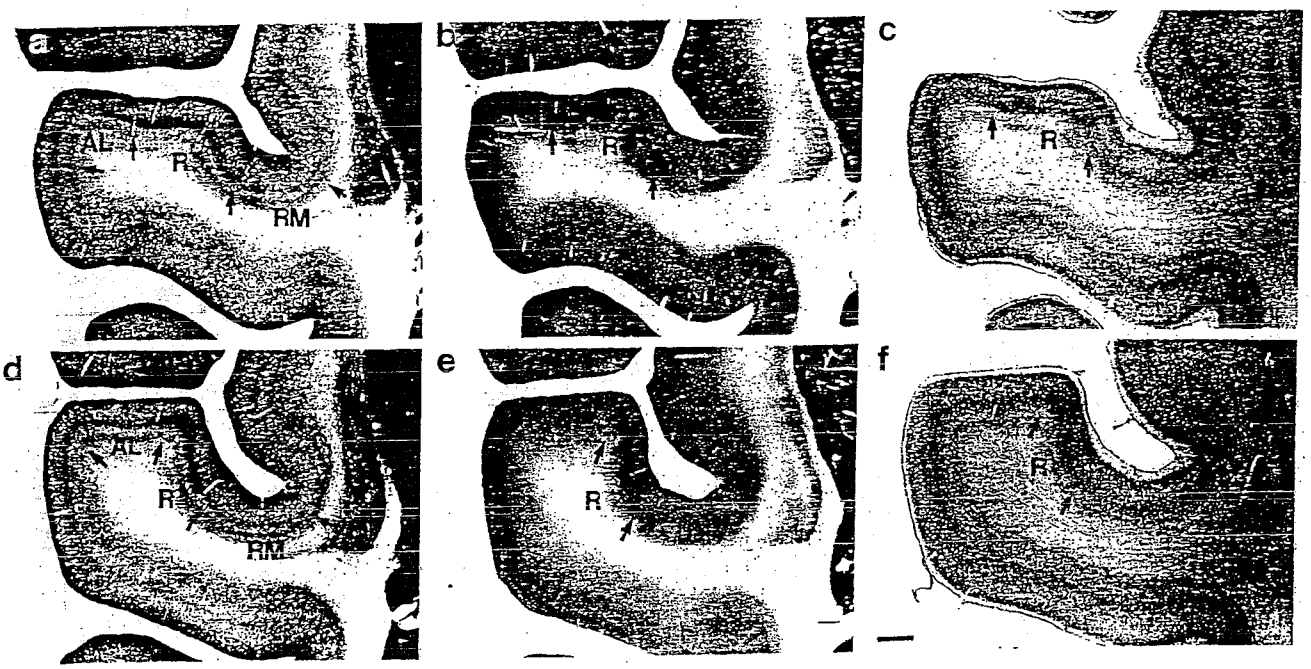

Fig. 5. The architecture of the rostral area (R) and surrounding cortex. a–c are coronal sections through the caudal half of R; d–f are through the rostral half of R. Sections a and d, AchE; b and e, CO; c and f, Nissl. Arrows mark the estimated extents of R, the anterior lateral field (AL), and the rostromedial field (RM). Note the electrode tract and microlesion in b and c. Scale bar = 1 mm and applies to a–f.

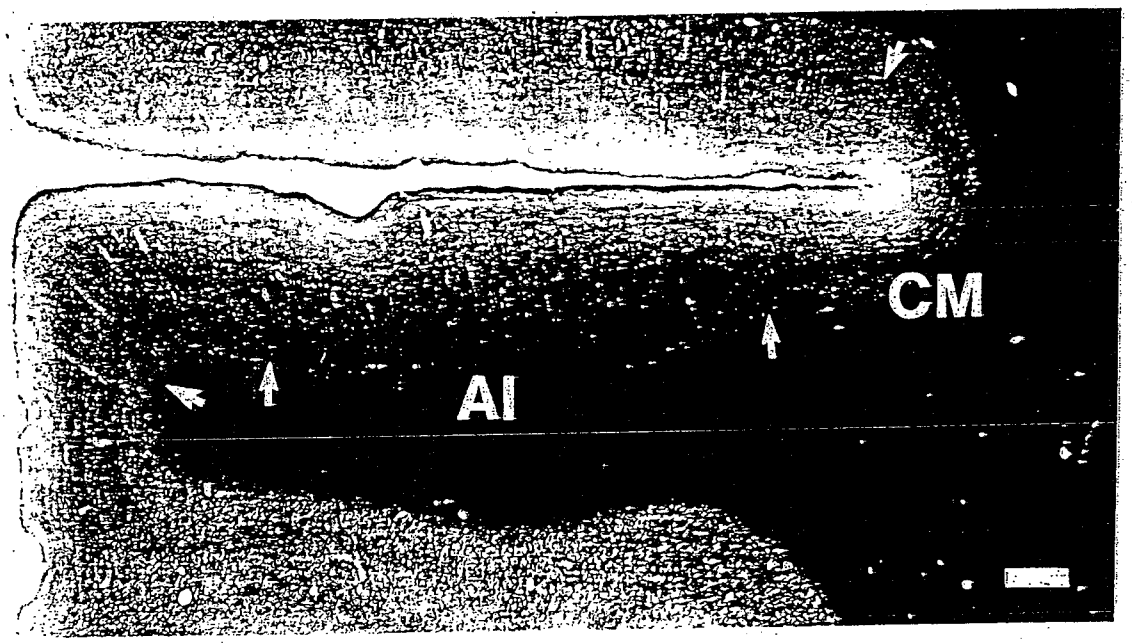

Fig. 6. The myeloarchitecture of AI and surrounding cortex. A coronal section through the rostral half of AI. Note the dense myelination in AI. Arrows mark the borders of AI, the caudomedial field (CM), and the posterolateral field, PL (see Fig. 4). Scale bar = 0.5 mm.

sumptive auditory fields by location and architectonic features. One such area is the caudomedial field, CM, first described by Merzenich and Brugge ('73) as cortex with deeply stained cells in layer IV and neurons responsive to tones with best frequencies largely in the high frequency range. We found cortex medial to AI in the fundus of the lateral fissure to have deeply stained neurons in layers IV and VI, and moderate levels of CO and AchE expressed in these same layers (Figs. 4 and 7). Thus, CM has architectonic characteristics of sensory cortex, but they are not so

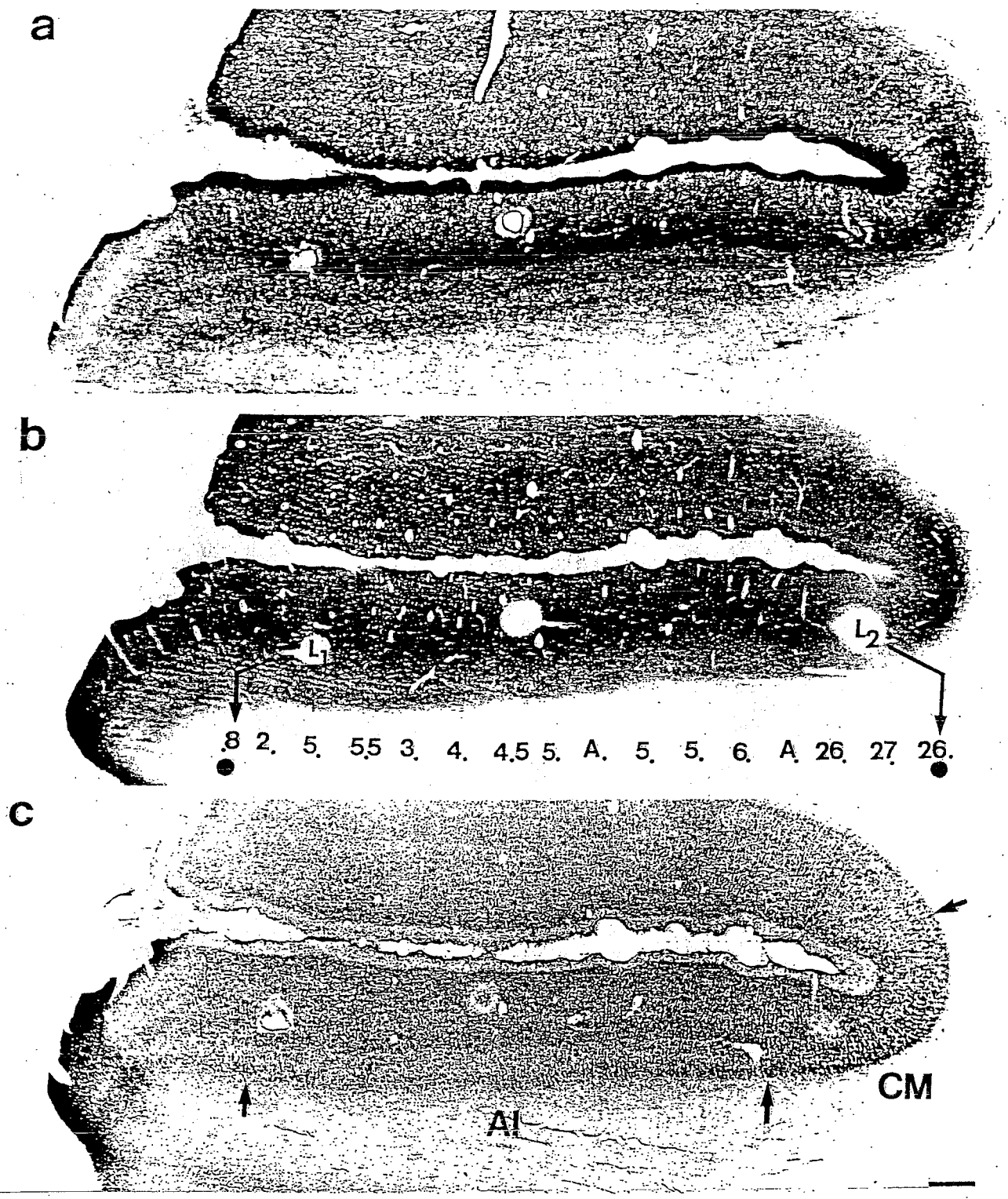

Fig. 7. The relation of best frequencies along a row of recording sites to the architecture of AI. Three adjacent coronal brain sections through the midportion of AI were processed for AchE (**a**), CO (**b**), or Nissl (**c**). In each section, two electrolytic microlesions are apparent near the lateral (L_1) and medial (L_2) boundaries of AI. The lesions mark the first and last recording sites along a sequence in a horizontal electrode penetration. The best frequencies in kH_Z of neurons at each recording site are indicated below the electrode tract. At site A, neurons were auditory, but a best frequency was not determined. Arrows in c mark the borders of AI and CM. A third microlesion in the middle of AI is from another electrode penetration. Scale bar = 0.5 mm and applies to a–c.

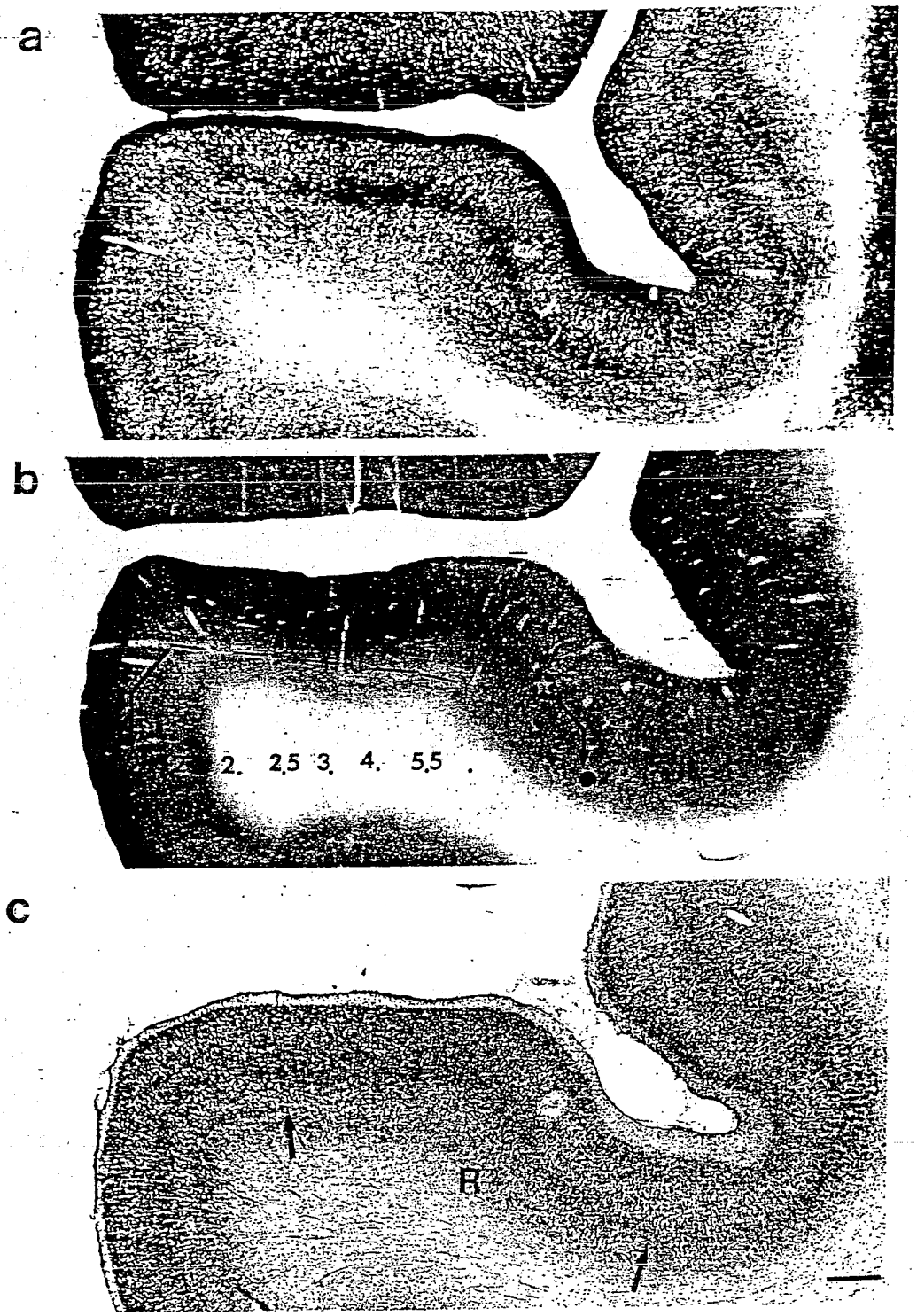

Fig. 8. The relation of best frequencies along a row of recording sites to the architecture of R. Three adjacent coronal sections through the midportion of R were processed for AchE (**a**), CO (**b**), or Nissl (**c**). A dashed line in b marks the course of an electrode penetration ending in a microlesion (L and circled star). The best frequencies in kH_Z for neurons at recording sites along the electrode penetration are indicated in an expanded row below (bent arrows). Dots mark three unresponsive sites. The large dot corresponds to the end of the penetration at the microlesion. The microlesion is apparent in a and c. Arrows in c mark the architectonic extent of R. Scale bar = 0.5 mm and applies to a–c.

pronounced as in AI and R. We also found, as did Merzenich and Brugge ('73), that neurons in CM responded well to tones, and had best frequencies in the high frequency range (Fig. 7). Cortex with these architectonic and physiological features was located medial to AI, extending somewhat onto the upper bank of the lateral fissure. However, the present CM does not include cortex caudal to AI, and thus it is somewhat smaller than the CM indicated by Merzenich and Brugge ('73). Instead, we refer to cortex caudal to AI, which has less differentiated layers, as the caudal area or region C. Layers IV and VI are well developed in cortex lateral to AI, but these layers are less pronounced in Nissl preparations than in AI or CM. Layer IV is somewhat darker in AchE and CO preparations than surrounding nonprimary cortex. Merzenich and Brugge ('73) referred to much of this region of cortex as the lateral field, but we refer to it as the posterior lateral field, PL, to distinguish it from more anterior cortex along the lateral border of R that we term the anterior lateral field or region, AL. While AL resembles PL in overall appearance, layer IV seems thicker and denser in AL. Cortex medial to R has a less distinct layer IV in all three preparations (Fig. 5) than R or even CM, and we refer to this rostromedial region as RM. Cortex immediately rostral to R had somewhat more pronounced architectonic features with layers IV and III being well differentiated, but less so than in R. We tentatively refer to this region as rostrotemporal cortex, RT. Finally, cortex on the surface of the superior temporal sulcus is distinct from PL by having a less dense band of AchE and CO in layer IV (Fig. 4).

Cortical connections of auditory cortex

Cortical connections of auditory cortex were investigated by placing injections of WGA-HRP and fluorescent tracers in and around AI at sites of known frequency representation. Because of our lateral approach for recording electrodes, most injections were placed in more accessible cortex near the lateral edge of AI. However, injections in two cases involved deeper portions of AI, and they best reveal the connections of AI. In one of these, case 91-73 (Fig. 9), injections of WGA-HRP (Fig. 9A), DY and FB were placed at high, middle, and middle-low frequency representations in AI. The injection of WGA-HRP, in cortex largely devoted to frequencies in the 15–20 kHz range, was large and included half of the width of AI. The lateral border of AI was slightly involved in the injection site (Fig. 10a), but almost all of the injection was in AI and the resulting pattern of label can be expected to reflect the connections of AI. Regions of ipsilateral cortical label included portions of AI around the injection site, especially rostromedially and caudolaterally along the lines of isorepresentation, and locations in nearby regions of cortex. One focus of dense label was in the rostral portion of R in the inferior limiting sulcus where higher frequencies are represented. Other foci of label were scattered medial to R in RM, medial and caudal to AI in CM and C, and lateral to AI in PL. A more distant lateral focus of label was in cortex on the upper lip of the superior temporal sulcus. Several locations lateral to R and AI were sparsely labeled.

In another case, a smaller injection of WGA-HRP was placed in a portion of AI deep in the fissure in a portion devoted to higher frequencies in the 20–30 kHz range (Fig. 11A). The injection core was largely in AI, but it slightly invaded CM. Again, dense label in cells and fine processes was located in adjacent parts of AI, this time in a zone extending caudally from the injection site along presumed lines of isofrequency. Another zone of dense label was located rostrally in R along the bank of the inferior limiting sulcus in cortex expected to represent high frequencies. Small foci of label were in CM and along the caudolateral border of AI. The results from these two cases suggest that the major connections of AI are intrinsic, largely along lines of isofrequency, and with tonotopically matched portions of R. Connections with medially and laterally adjoining regions of cortex also seem likely, but uncertainties exist because such connections were not revealed by the smaller injection. Further information on the connections of AI was obtained from other cases. First, in those cases (case 91-73, Fig. 9B and case 91-52, not shown) with injections that involved both portions of lateral AI and PL, labeled cortex was found in AI, R, RM, CM, adjacent parts of PL, AL, and cortex of the upper bank of the superior temporal sulcus. Thus, AI injections involving both AI and PL labeled all of the presumptive targets of AI. Second, injections in a presumptive target of AI, PL (Fig. 11B) or PL plus some of AL (Fig. 12), densely labeled AI. From these results, it seems reasonable to conclude that AI has (1) prominent and broadly distributed intrinsic connections extending, in part, along isofrequency lines, (2) dense connections with locations in R, (3) connections with the PL-AL region along the lateral border of AI and R, and (4) connections with CM and RM. Connections with other regions including cortex of the upper bank of the superior temporal sulcus and cortex caudal to AI seem possible, but more evidence is needed.

The injections in cortex along the lateral border of AI included cortex that responds to auditory stimuli and has connections with AI. Connection patterns revealed by the injections in PL (Fig. 11B) or PL plus some AL (Fig. 12) indicate that this cortex also has connections with R, RM, CM, and much of the superior temporal gyrus lateral to PL. Thus, a large expanse of cortex around and lateral to AI and R has auditory connections.

Injections in AI labeled neurons and terminals in supragranular and infragranular layers in other adjacent parts of AI. Both types of label were also largely in supragranular and infragranular layers in R. Injections in PL and adjoining cortex labeled neurons in supragranular and infragranular layers in AI, R, and cortical fields around AI and R.

We also reconstructed patterns of label in contralateral cortex after auditory cortex injections. The large injection of WGA-HRP centered in lateral AI of the left hemisphere (Fig. 9) produced dense label in the comparable and more medial location in AI of the right hemisphere (Fig. 13). Other zones of much less dense label were in PL, CM, and R. The injection in medial AI (Fig. 11) labeled regions of medial AI and the adjoining part of R in the contralateral hemisphere, as well as part of CM (Fig. 14). Thus, the major callosal connections of AI appear to be with matched parts of AI, while sparser callosal connections appear to include other parts of AI, R, and perhaps CM and PL. Callosally projecting neurons and terminations were largely confined to supragranular layers (Fig. 10b).

Injections in cortex lateral to AI and along the lateral border of AI provided further evidence on the nature of interhemispheric auditory callosal connections. In case 91-73, closely spaced injections of FB and DY were placed in lateral AI and adjoining PL in locations activated by middle and middle-low frequencies (Fig. 9B). The injections produced slightly overlapping zones of label that were displaced rostrocaudally in contralateral AI (Fig. 13) The

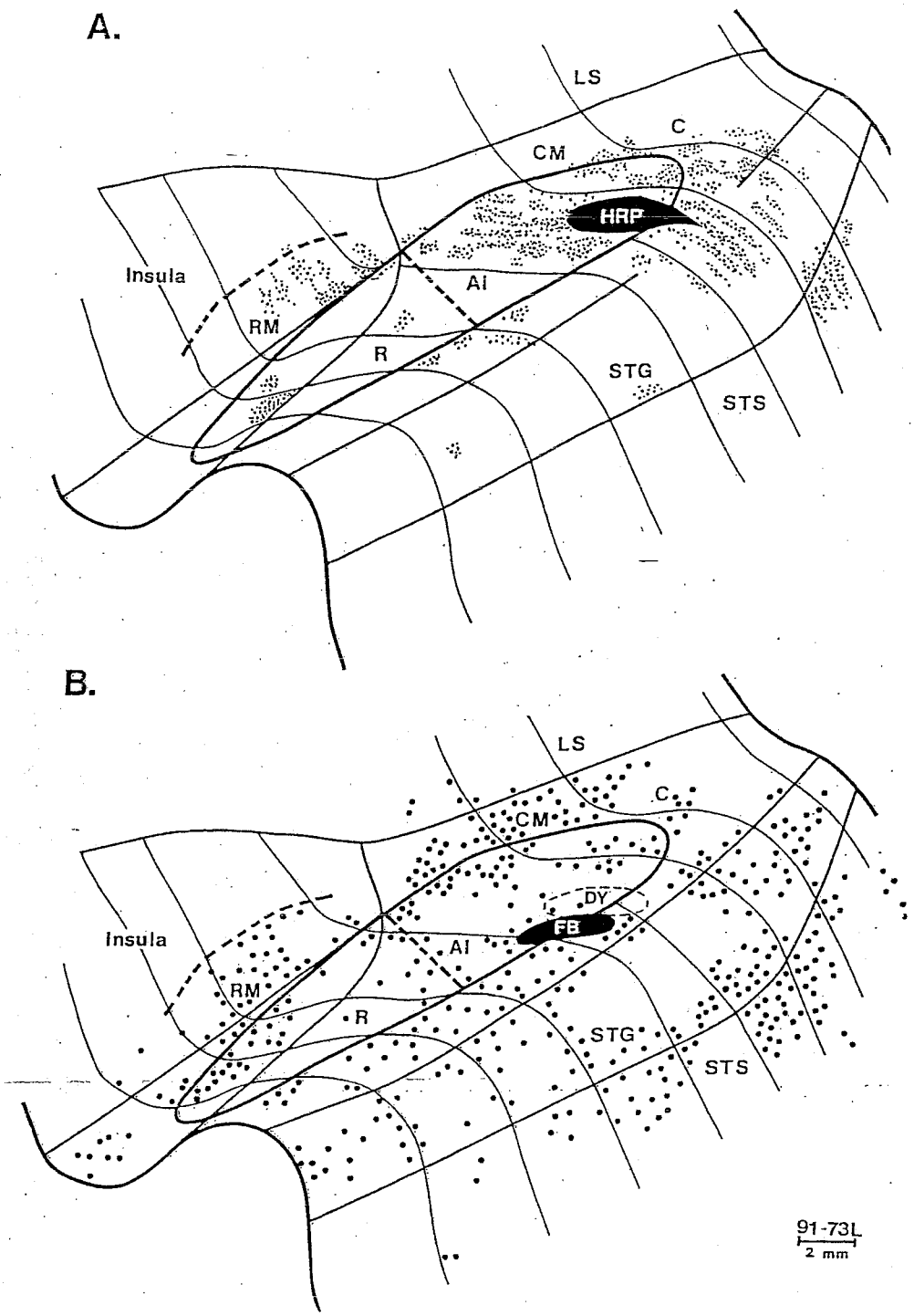

Fig. 9. Connections of auditory cortex in case 91-73. An injection of WGA-HRP was placed in AI and the fluorescent dyes diamidino yellow (DY) and fast blue (FB) were injected along the lateral border of AI. The WGA-HRP was injected in cortex responsive to 15–20 kH_z; DY, 10 KH_z; FB, 5 KH_z. A: The injection site (black) and transported label (dots) after the WGA-HRP injection. The larger dots represent labeled neurons while smaller dots indicate labeled terminals. B: Locations of neurons labeled with FB (dots) and the injection sites of DY (dashed oval) and FB (black oval). The DY neurons (not shown) and FB neurons overlapped extensively. The slightly unfolded reconstructions are from the frontal-dorsolateral perspective of the left hemisphere. Compare with Figure 1. LS, lateral sulcus; C, caudal auditory area; CM, caudomedial auditory area; STG, superior temporal gyrus; STS, superior temporal sulcus. Dashed lined mark the estimated border between AI and R, and the dorsal border of RM.

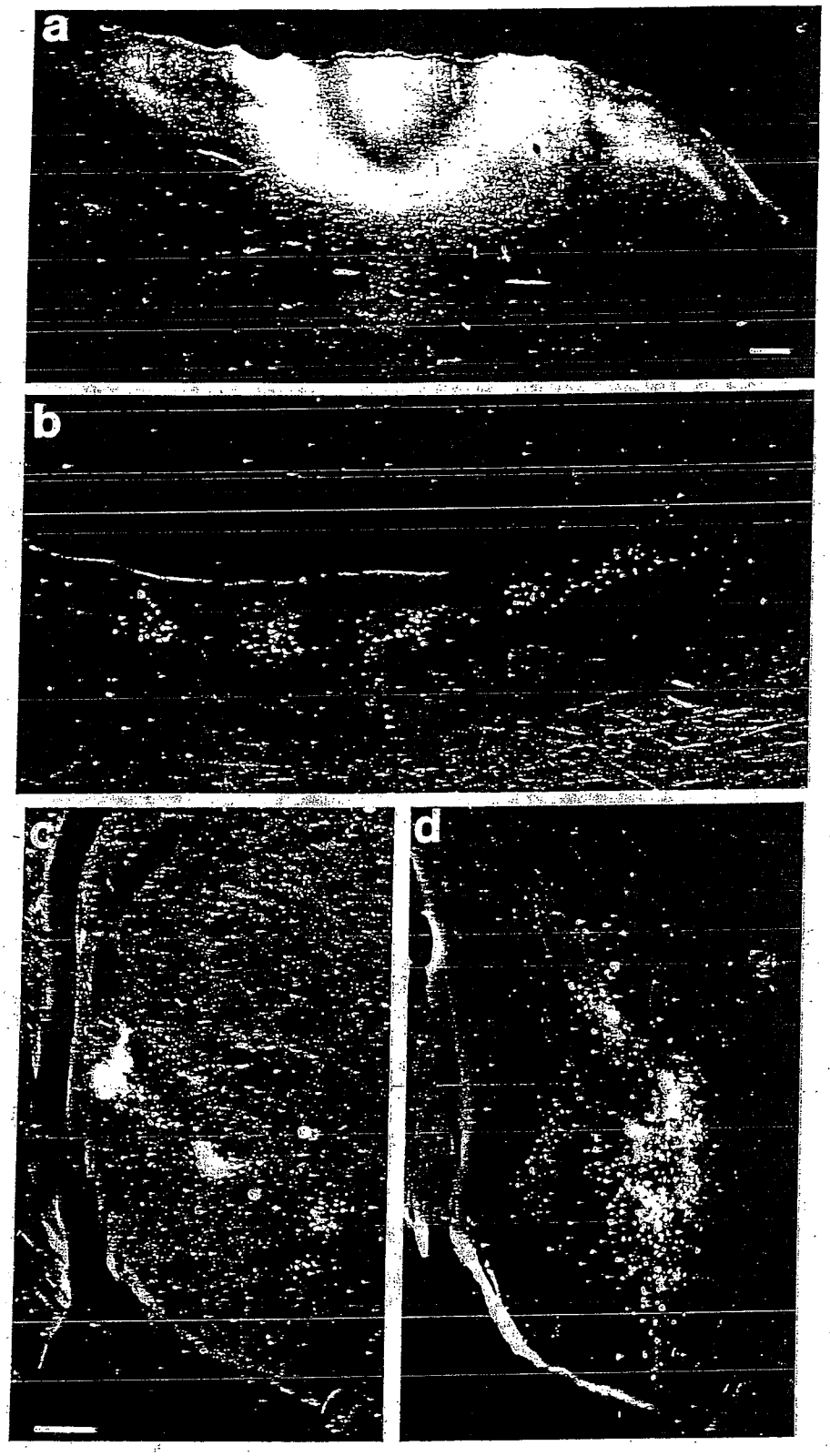

Fig. 10. Darkfield photomicrographs of an injection site of WGA-HRP and transported label in coronal brain sections. **a:** An injection site and transported label in AI of case 91-73; compare with Figure 9A. **b:** Scattered clumps of labeled neurons in AI contralateral to the AI injection site in case 91-73; also see Figure 13. **c:** Clumps of labeled neurons and terminals in the medial geniculate complex in case 91-73; compare with Figure 16. **d:** Label in the medial geniculate complex in case 90-64; compare with Figure 17. Scale bars = 0.5 mm.

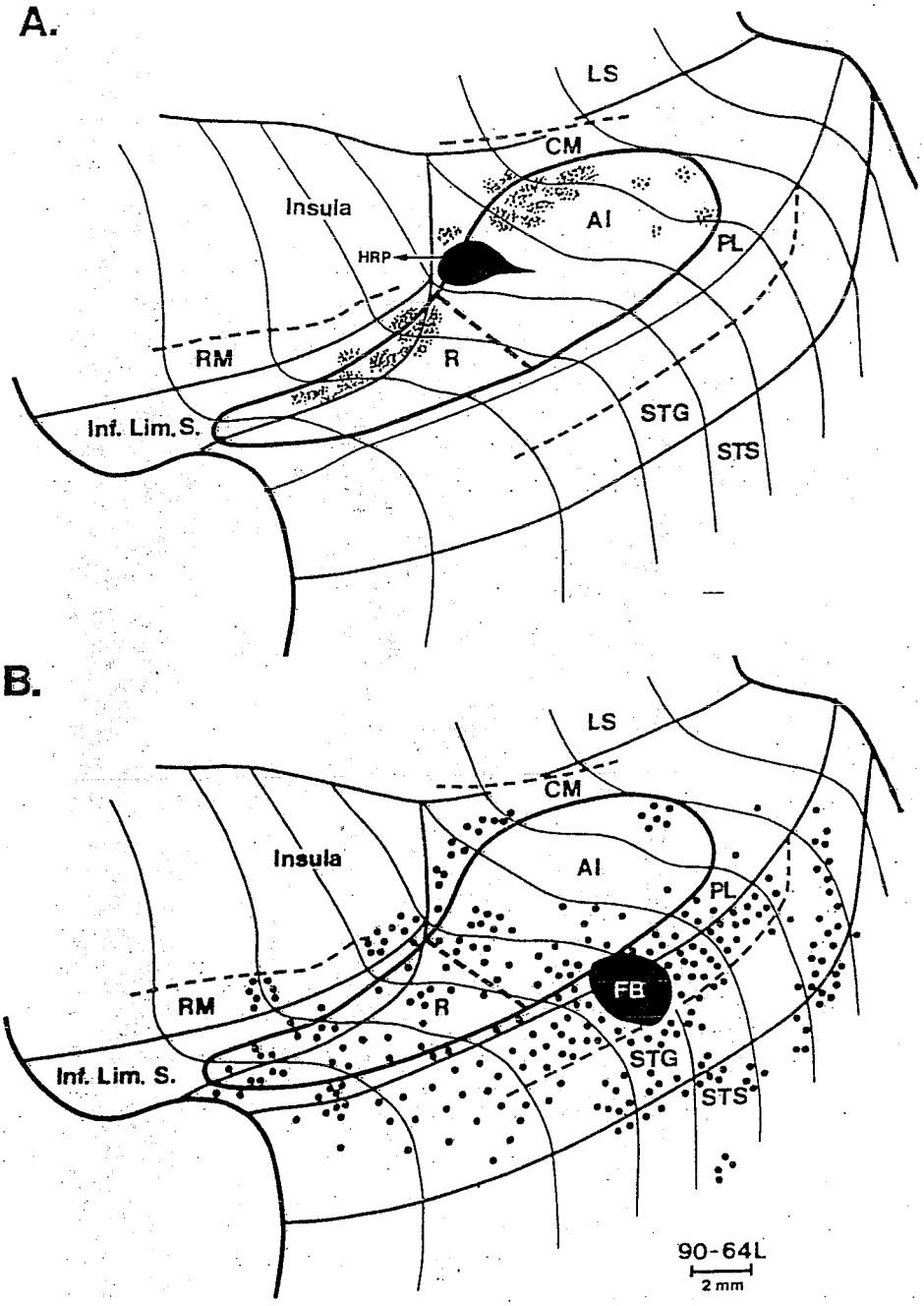

Fig. 11. Connections of auditory cortex in case 90-64. An injection of WGA-HRP was placed medially in AI in cortex responsive to tones in the 20–30 kH_z range and an injection of fast blue (FB) was placed lateral to AI in cortex responsive in the 0.5–2 kH_z range. **A:** The injection site and transported label after the WGA-HRP injection. **B:** The injection site and transported label after the FB injection. Inf. Lim. s., inferior limiting sulcus. Other conventions as in Figure 9.

zones of contralateral label after the injections that involved both AI and PL included AI, PL, R, RM, and CM, perhaps as a result of involving PL in the injections or possibly because fluorescent tracers sometimes reveal more connections than WGA-HRP. In another case (90-64), an injection of FB in anterior PL (Fig. 11B) labeled neurons in contralateral auditory cortex over much of PL, parts of AI and R, CM, and cortex lateral to PL and AL. Thus, the callosal connections of PL include PL and other auditory fields that can be regarded as higher (lateral cortex) or lower (AI) in a processing sequence.

The architecture and cortical connections of the auditory thalamus

The brain sections stained for cell bodies or processed for CO were most useful in distinguishing subdivisions of the auditory thalamus (Fig. 15). Just medial to the lateral

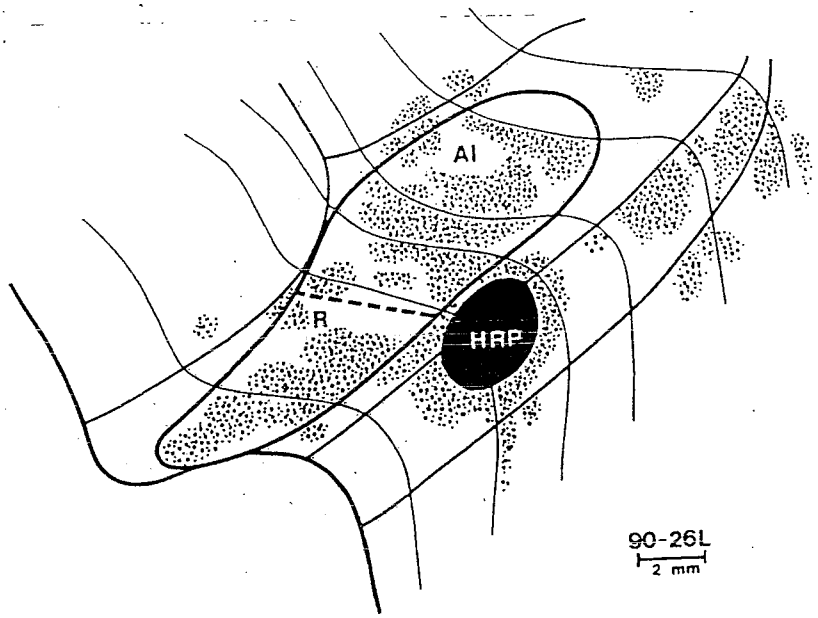

Fig. 12. Cortical connections after an injection of WGA-HRP into cortex lateral to AI and R at the PL-AL junction. Case 90-26. Conventions as in Figure 9.

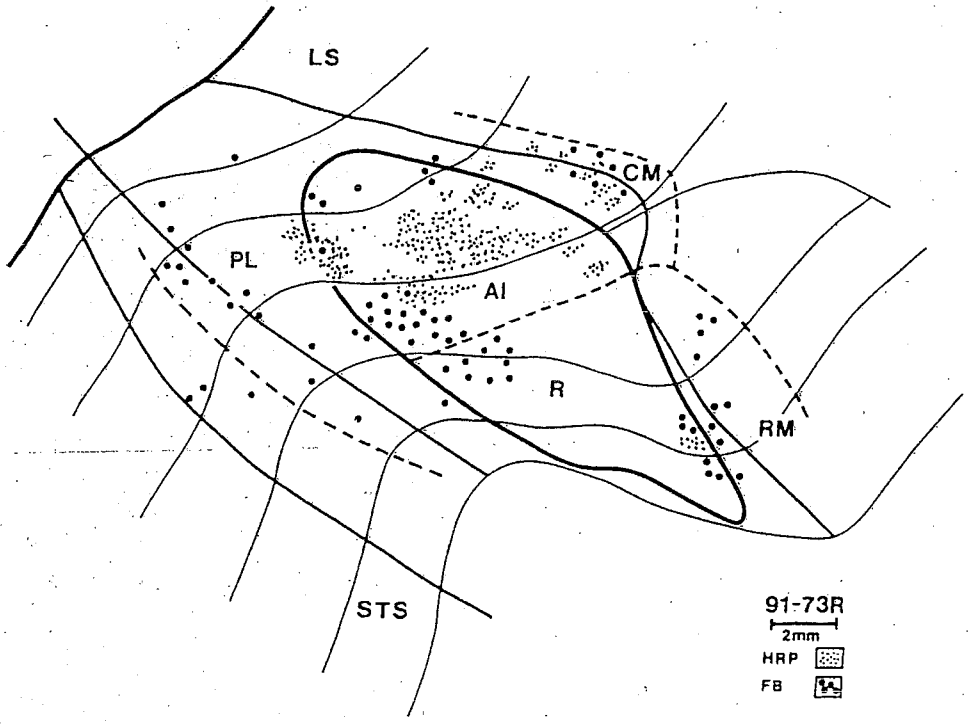

Fig. 13. Callosal connections of auditory cortex in case 91-73. An injection of WGA-HRP into the opposite AI labeled neurons and terminals (small dots) in AL, PL, and CM, while an injection of FB at the AI-PL border resulted in a somewhat more extensive distribution of labeled neurons (large dots). Left hemisphere. See Figure 9 for injection sites and conventions.

geniculate nucleus and the inferior pulvinar, a large ventral nucleus (MG_V) of the medial geniculate complex was identified as a region with densely packed, small neurons and high levels of CO activity. The ventral nucleus was largest and most conspicuous rostrally (Fig. 15C and F), where it extended dorsoventrally across the medial geniculate complex. More caudally, the dorsal nucleus (MG_D) of the complex was apparent as a dorsolateral region with larger, more scattered neurons and lower levels of CO activity (Fig. 15A and D). The transition from the densely packed

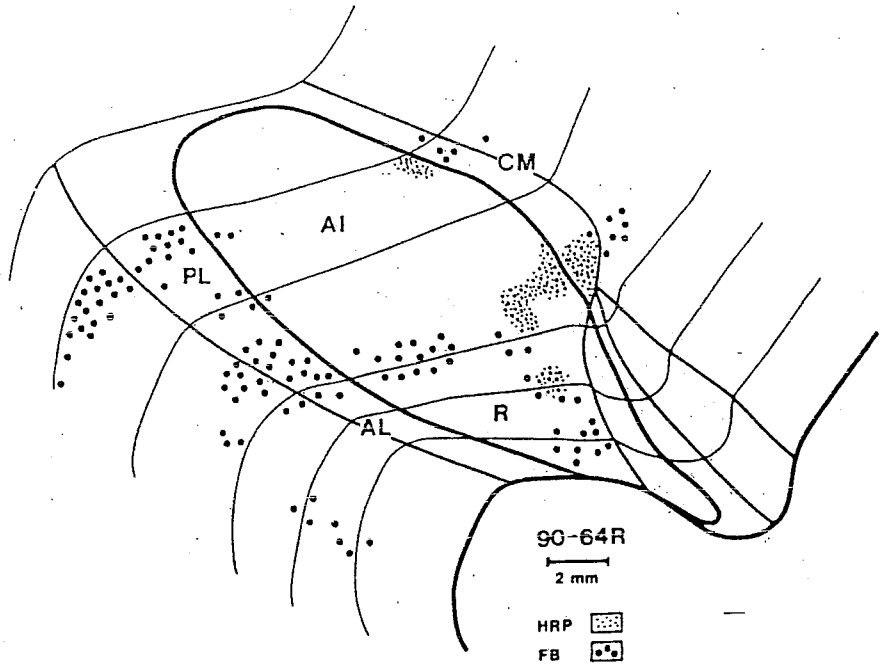

Fig. 14. Callosal connections of auditory cortex in case 90-64. An injection of WGA-HRP in the mediorostral portion of contralateral AI labeled terminals and neurons (smaller dots) mediolaterally across AI and in adjoining parts of R and CM. An injection of FB in contralateral PL labeled neurons (large dots) in PL and other regions. See Figure 11 for injection sites. Conventions as in previous figures.

neurons of the ventral nucleus to the more scattered neurons of the dorsal nucleus was not always abrupt, and it was typically difficult to determine an exact border. Perhaps because of this difficulty, our ventral nucleus is larger than the ventral nucleus depicted for macaques by Jones ('85) and our dorsal nucleus is smaller and more confined to the caudal part of the complex. Just medial to the ventral nucleus, the medial or magnocellular nucleus (MG_M) was apparent as a region of large, scattered cells that were associated with high but uneven levels of CO activity. The suprageniculate nucleus consists of a group of large, darkly stained neurons just dorsomedial to the medial geniculate complex. A small region of scattered neurons just dorsal to the rostral part of the complex and ventrolateral to the ventroposterior nucleus is generally considered part of the posterior "nucleus" or complex (Jones, '85). Both these portions of the posterior nucleus, Po, and the suprageniculate nucleus have been associated with the auditory system by connections with auditory cortex (see Jones, '85).

Thalamocortical connections. The results indicate that AI receives input from all three nuclei of the medial geniculate complex. All injections involving AI densely labeled the ventral nucleus, but labeled cells were also found in the medial and dorsal nuclei. Perhaps the clearest results were from case 91-73 (Fig. 16) where an injection of WGA-HRP was nearly completely confined to AI. Labeled neurons and fine processes judged to be terminals were conspicuous in dorsomedial MG_V throughout the rostrocaudal extent of the nucleus. Other labeled neurons and terminals were in MG_M and a few of the most caudally labeled neurons in the complex appeared to be in MG_D. A few labeled neurons were scattered in the posterior nucleus, Po, and in the medial pulvinar. Results after an injection of WGA-HRP in the rostromedial portion of AI (Fig. 17) were similar in that medial parts of MG_V and lateral parts of MG_M were densely labeled, while some dorsally located label appeared to be in MG_D. A few labeled neurons were in Po. These results, together with those from other injections involving AI, support the conclusions that the major thalamic connections of AI are with MG_V, but substantial connections also exist with MG_M. MG_D appears to be sparsely connected with AI, and a few neurons in Po, the suprageniculate nucleus, and the medial pulvinar appear to project to AI.

The present cases also provide evidence that the medial geniculate complex projects to cortex just lateral to AI. In case 90-64, for example, a large injection of FB was placed in PL just outside the rostrolateral border of AI. Labeled neurons were evident in all three divisions of the medial geniculate complex (Fig. 17). While the distribution of label in the medial geniculate complex resembles that of AI injections, the suprageniculate nucleus and Po were more densely labeled than after AI injections. Our WGA-HRP injection in cortex just lateral to R at the PL-AL junction also labeled MG_V, MG_M, MG_D, SG, and Po (not shown). Thus, the medial geniculate complex appears to project to both AI and cortex along the lateral margin of AI and R.

Since our injections were placed at sites where the best frequencies of neurons were determined, the resulting patterns of thalamic connections provide information on the presumptive tonotopic organization of the nuclei of the medial geniculate complex. In case 91-73, injections of three different tracers were centered in cortex responsive to higher (15–20 kH_Z), middle (10 kH_Z) and lower (5 kH_Z) frequencies, and thalamic label resulting from the injections in the cortex responsive to the higher and the lower frequencies is shown in Figure 16. In MG_V, neurons projecting to cortex activated by higher frequencies were

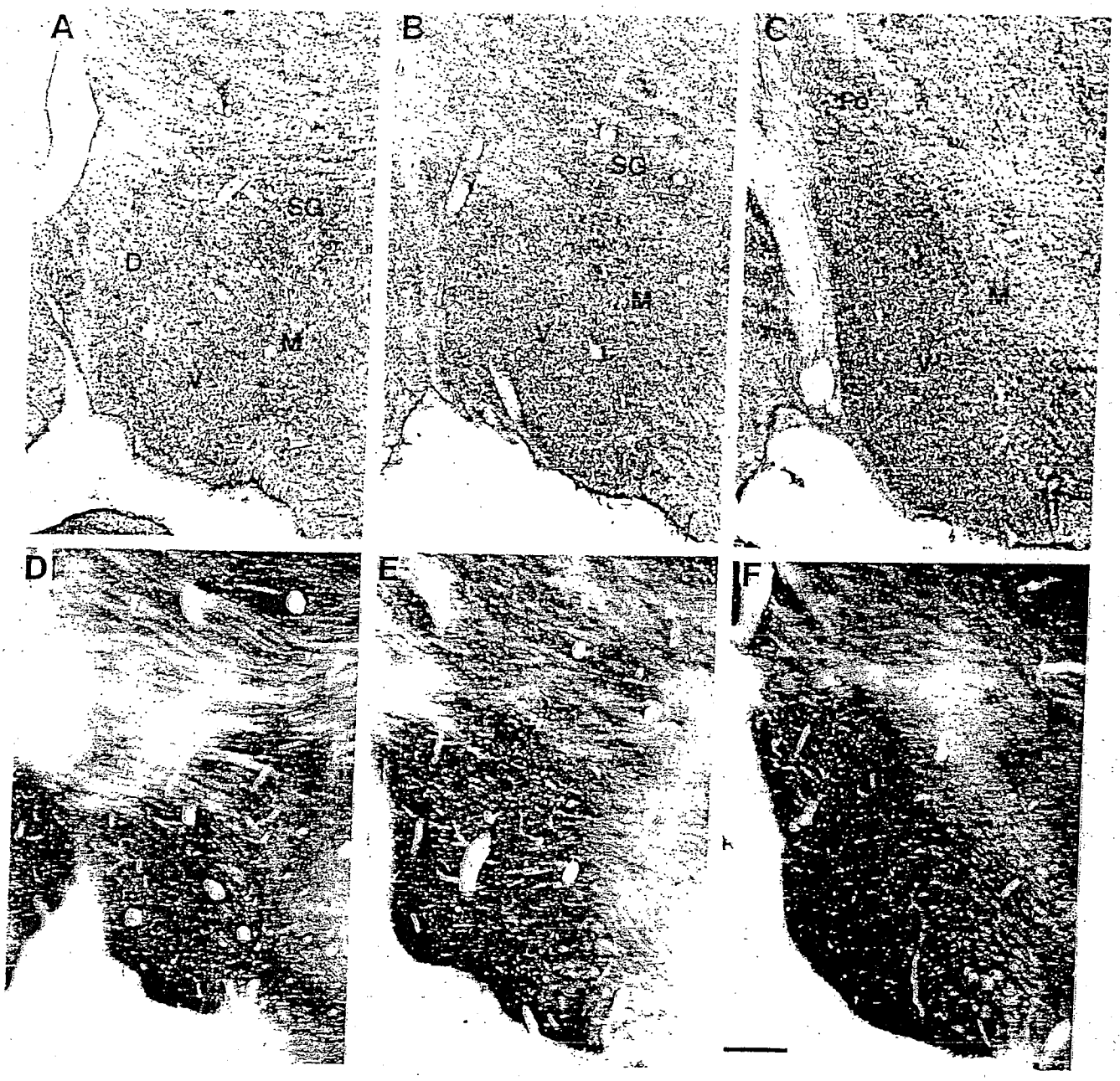

Fig. 15. The architecture of the medial geniculate complex. Coronal sections in A–C are stained for Nissl substance and they are matched for level below with sections D–F processed for CO. Sections A and D are 0.75 mm from the caudal pole of the complex; sections B and E are 0.5 mm more rostral, and section C and F are 0.75 mm more rostral and near the rostral pole of the complex. Dorsal (D), ventral (V), and medial (M) nuclei of the medial geniculate complex are indicated. Suprageniculate nucleus, SG; posterior nucleus, PO. Scale bar = 0.5 mm and applies to A–F.

dorsal to those projecting to cortex related to the lower frequencies. Neurons projecting to the middle frequency zone (not shown) were centered between these two populations, but the populations overlapped considerably. Similar results were obtained from case 90-64, where an injection of WGA-HRP was placed in cortex activated by higher tones (20–30 kH_Z) and fast blue was injected in cortex activated by lower tones (.5–2.0 kH_Z). Again the neurons labeled by the injections in cortex responsive to higher frequencies labeled more dorsomedial portions of the MG_V.

DISCUSSION

The present results indicate that there is a distinctive koniocortical zone of auditory cortex on the lower bank of the lateral sulcus of macaque monkeys that can be divided on the basis of tonotopic patterns into a primary area, AI, and a rostral area, R, as previously proposed by Merzenich and Brugge ('73). Most or all of the cortex immediately surrounding AI and R appears to be auditory, judging from limited recording and connections with AI, and we have

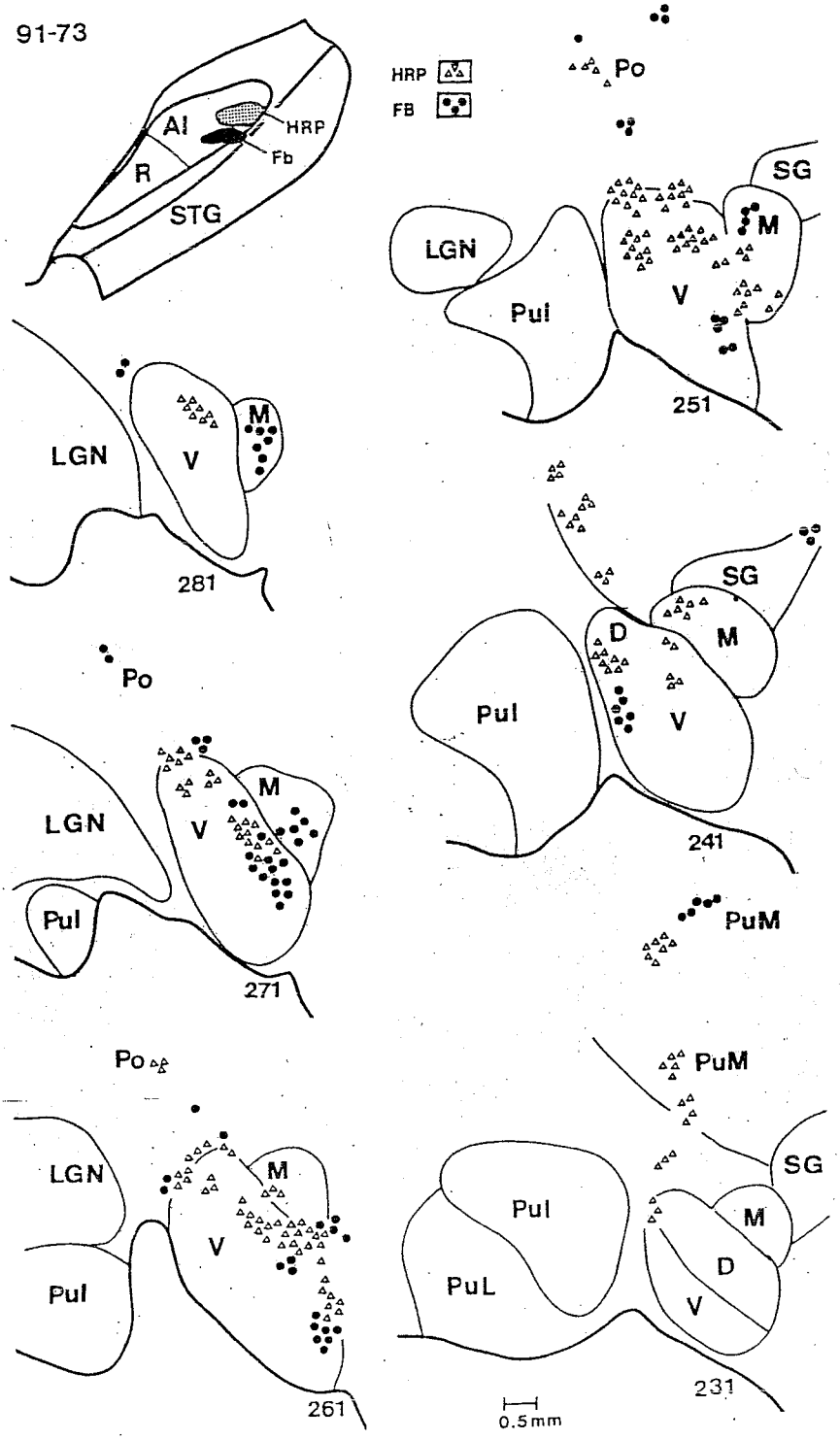

Fig. 16. Thalamic label after injections in auditory cortex in case 91-73. The figure on the upper left shows the positions of a WGA-HRP injection in a portion of AI that was activated by tones in the range of 15–20 kHz and a fast blue (Fb) injection near the AL-PL border in cortex responsive to 5 kHz (see Figure 9 for details). Drawings of a caudorostral series of 50 μm coronal brain sections through the medial geniculate complex are below. Neurons labeled by WGA-HRP, triangles; neurons labeled by FB, dots. Dorsal (D), ventral (V), and medial (M) nuclei of the medial geniculate complex are indicated. LGN, lateral geniculate nucleus; PuI, inferior pulvinar; PuL, lateral pulvinar; PuM, medial pulvinar; Po, posterior nucleus; SG, suprageniculate nucleus. Brain sections are numbered in sequence.

proposed several tentative subdivisions of this cortex based on architectonic distinctions, connections with AI, tonotopic patterns, and evidence from previous studies on macaques (Merzenich and Brugge, '73) and other monkeys (e.g., Morel and Kaas, '92). Both AI and cortex immedially lateral to AI have tonotopically organized connections with

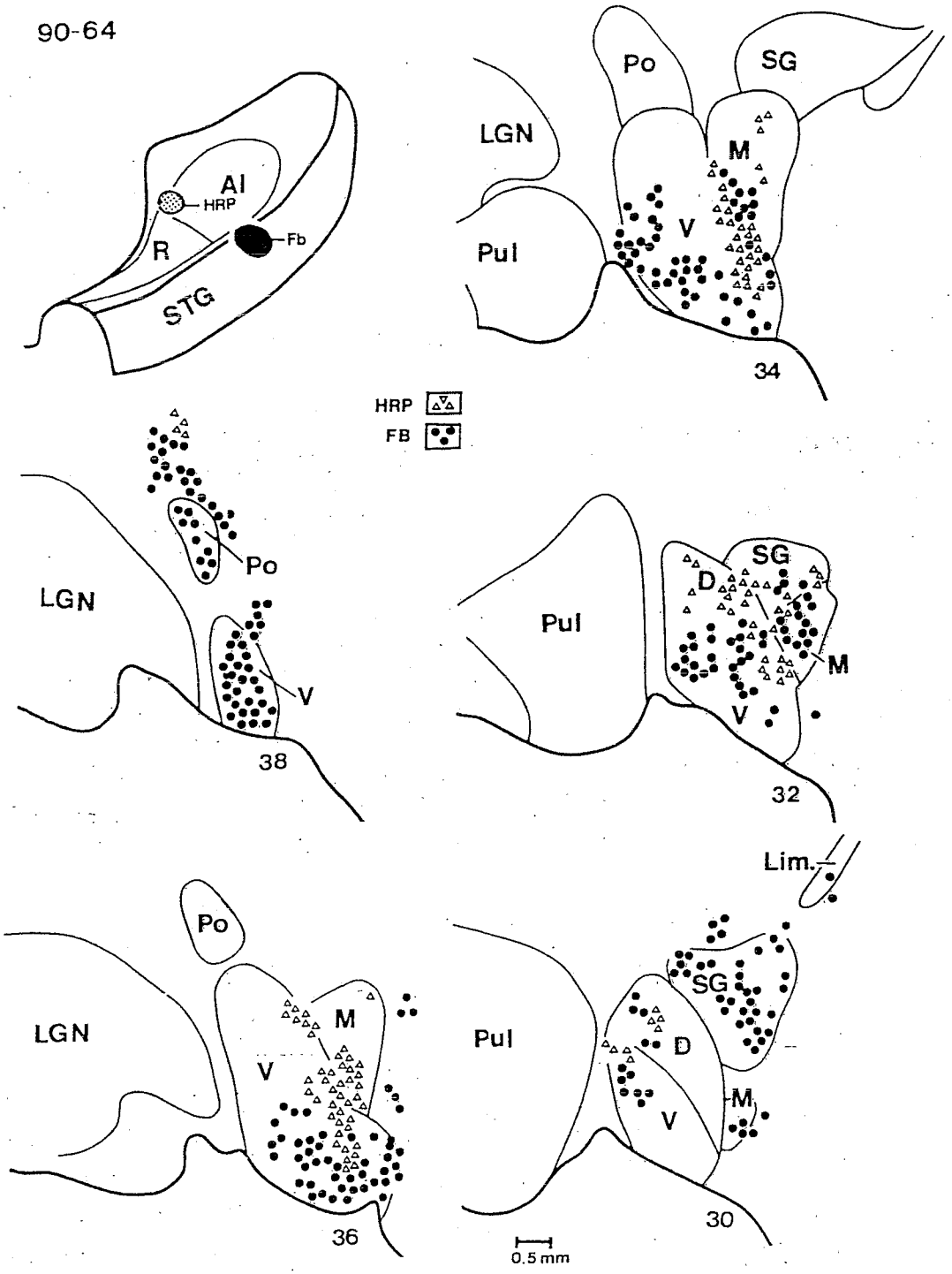

Fig. 17. Thalamic label after injections in auditory cortex in case 90-64. The WGA-HRP injection was in cortex responsive to 20–30 KH_z tones while the FB injection was in cortex responsive to 0.5–2.0 KH_z. See Figure 11 for other details of injection sites. Lim., limitans. Other conventions as in Figure 16.

the ventral nucleus of the medial geniculate complex. Major conclusions are discussed below.

The organization of auditory cortex in macaques

Our present conclusions on how auditory cortex is subdivided and tonotopically organized are summarized in Figure 18A. A broad zone of cortex on the lower bank of the lateral sulcus and extending rostrally along and into the inferior limiting sulcus is characterized by architectonic features that are associated with primary sensory representations. Thus, this cortex has a well developed granule cell layer that is densely packed with small neurons and tends to merge with layer III. The region is densely myelinated,

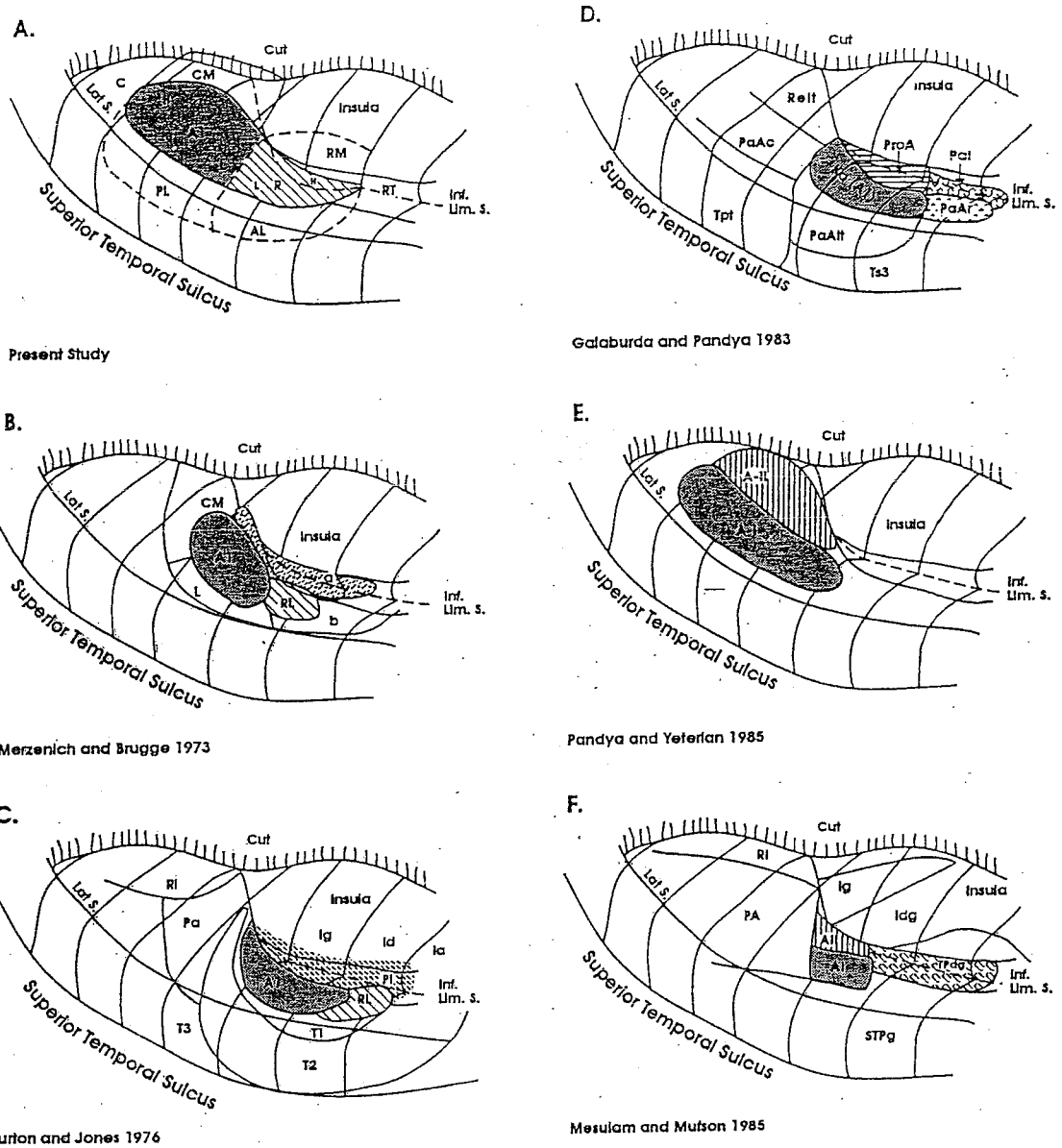

Fig. 18. Present and previous concepts of the locations of subdivisions of auditory cortex illustrated on a standard dorsolateral surface view of the superior temporal plane for ease of comparison. **A:** Our results support the earlier conclusion of Merzenich and Brugge ('73) that a large primary-like region consists of two fields, AI or the traditional primary field and a rostral field (R) which corresponds to their rostrolateral field (RL). AI and R each represent tones from high (H) to low (L) as indicated. Bordering cortex includes caudal (C), caudomedial (CM), posterior lateral (PL), anterior lateral (AL), rostromedial (RM) and rostrotemporal (RT) fields. See text for further details. **B:** Merzenich and Brugge ('73) defined AI, the rostrolateral field (RL), the caudomedial field (CM), the lateral field (L), and fields "a" and "b." **C:** Burton and Jones ('76) studied thalamocortical connections and cortical architecture and subdivided auditory and surrounding cortex into an AI and RL (after Merzenich and Brugge, '73), first, second, and third temporal fields (T1, T2, and T3), postauditory field (Pa), a parainsular auditory field (Pi), a retroinsular field (RI), and granular (Ig), dysgranular (Id), and agranular (Ia) insular fields. **D:** Galaburda and Pandya ('83) modified and simplified an early description of Pandya and Sanides ('73) and designated a large auditory koniocortical area Ka, which they considered to be AI, proisoauditory cortex (ProA) is medial to AI and was considered to be the second auditory area, A-II. Auditory parakoniocortical areas are caudal (PaAc), lateral (PaAlt), and rostral (PaAr) to AI. Tpt is the temporoparietal area. Relt, retroinsular. **E:** Pandya and Yeterian ('85) illustrated AI (Ka) and A-II (pro A) as larger and more caudal fields than did Galaburda and Pandya ('83). **F:** Mesulam and Mufson ('85) divided the auditory region in primary (AI) and secondary (A-II) fields. Other subdivisions included granular (Ig) and dysgranular (Idg) insular fields, a retroinsular field (RI), a superior temporal granular field (STPg), a temporopolar dysgranular field (TPdy), and a postauditory field (PA). Lat. S., lateral sulcus; Int. lim.s., inferior limiting sulcus.

its middle layers express CO and AchE, and resting levels of glucose use, measured with 2 deoxyglucose, are higher than in surrounding cortex. This architectonic zone can be subdivided into a caudal field, primary auditory cortex or AI, and a rostral field R largely on the basis of different patterns of tonotopic organization. High frequency tones are represented caudomedially in AI and rostromedially in R, while low frequency tones are represented rostrolater-

ally in AI and caudolaterally in R. Thus, the tonotopic progressions in each field are almost in opposite directions, and the two fields are roughly mirror-image reversals of each other in this respect. However, another possible interpretation of the physiological and architectonic results is that AI is a larger but partially split field, much as is V-II of monkeys (e.g., Allman and Kaas, '74). According to this possibility, a single central region, including parts of AI and R of Figure 18A, represents low tones, with successive semicircles of cortex, extending caudally, medially, and rostrally, representing successively higher tones. For the highest tones, the semicircles are discontinuous or split so that separate rostral and caudal zones are devoted to the highest tones.

We have previously considered the interpretation of AI and R together as a larger "AI" for owl monkeys (Morel and Kaas, '92), while concluding that the bulk of the evidence, including topographic connections between AI and R and slight architectonic differences, support the interpretation of two fields in these primates, as previously proposed by Imig et al. ('77). Nevertheless, we remain impressed with the architectonic similarities between AI and R, and we noted no clear architectonic border between the two fields in our coronal brain sections. In addition, although AI and R were interconnected, there was no marked difference in density and laminar pattern in these connections and those judged to be intrinsic in AI. Thus, it may be worthwhile to continue to evaluate the alternative hypothesis of a larger "split" AI containing both of the presently proposed primary-like fields, AI and R.

The most relevant previous observations on the identification of AI and R in macaques are those of Merzenich and Brugge ('73). These investigators (Fig. 18B) demonstrated the responsiveness of neurons in the two fields to tones, the mirror-image progressions of tonotopic order in the two fields, and the coextensiveness of the responsive region with koniocortex. They concluded that AI and R (their RL) were "very much alike cytoarchitectonically" but noted slight differences in that the upper layers of R were not as densely packed with cells and layer V was not as sparse.

In most respects, our observations are highly consistent with those of Merzenich and Brugge ('73). We extend R further rostrally and more into the inferior limiting sulcus than did Merzenich and Brugge ('73), but they mapped only the portion of R responsive to lower tones (up to about 7 kH_Z), while we found more rostral koniocortex responsive to high tones (up to about 32 kH_Z). In addition, our AI is larger and extends further caudally to occupy more of the lower bank of the lateral sulcus. In part, this could reflect more complete mapping of the caudal part of AI representing higher frequencies. In addition, the inclusion of brain sections processed for CO and especially for AchE greatly facilitated our architectonic analysis.

Other definitions of AI and R in macaques have been based on architectonic distinctions. We have depicted several of the most relevant previous descriptions in Figure 18 on a standard view for ease of comparison, though at the risk of not being completely accurate in our transposition (also see Walker, '37). Nevertheless, the figure indicates that AI, or auditory koniocortex, has been depicted as varying in location from largely caudal to largely rostral to the caudal end of the inferior limiting sulcus, and varying in size from a few square millimeters to four or five times that size. By position, it appears that previous investigators included much of R in AI and included much of AI in other areas. A problem for studies depending on an architectonic definition is the great similarity in appearance of AI and R, and, of course, the validity of this distinction can be questioned. But, the conclusions from previous studies also suggest that parts of R appear to some investigators to be more koniocortical in appearance than parts of AI. This problem of identification by architectonic criteria may be alleviated somewhat by the use of multiple histological and histochemical procedures, and stains for AchE seem especially useful. Curiously, auditory cortex in macaques has not been described as particularly expressive of AchE (e.g., Mesulam et al., '84), but AI is easily identified by dense AchE in cats (Wallace et al., '91) and immature rodents (Robertson, '87; Robertson et al., '91). Other procedures may be nearly as useful. For example, AI (and probably R) stains darkly when processed for parvalbumin immunoreactivity (Hashikawa et al., '91; Morino-Wannier et al., '92).

A review of early (e.g., Brodmann, '09; von Bonin and Bailey, '47) or more recent (see Fig. 18) architectonic studies of the auditory region of macaques reveals a diversity of opinion on how cortex surrounding the primary field is subdivided. Such diversity suggests that the distinguishing architectonic features of adjoining fields are not marked, and that without further experimental study, perhaps using microelectrode mapping, tracing of connections, and immunohistochemical approaches in combination, a further understanding and consensus is unlikely to emerge. We have tentatively labeled regions of cortex surrounding AI and R by locations as possible auditory areas as a guide for further study. The scheme is consistent with experimental observations from the present study and those of Merzenich and Brugge ('73), and follows our proposal for the organization of auditory cortex in New World monkeys which was based on connectional, electrophysiological, and architectonic evidence (Morel and Kaas, '92). A guiding assumption, supported by data from a limited number of recording sites in cortex surrounding AI and R in the present study and that of Merzenich and Brugge ('73), is that fields immediately surrounding AI and R have some degree of tonotopic organization, and that borders of adjoining auditory areas with AI and R have tonotopically matched or congruent borders. This assumption is consistent with known relations between adjoining auditory areas in other monkeys (Imig et al., '77; FitzPatrick and Imig, '80; Aitkin et al., '88; Luethke et al., '89; Morel and Kaas, '92) and mammals in general (see Luethke et al., '88), as well as between visual and somatosensory areas (see Kaas, '87). First, we propose that different auditory areas exist along the medial and lateral boundaries of AI and R with matched tonotopic progressions, and that these areas do not cap the caudal end of AI and the rostral end of R, but other auditory areas exist in these regions (Fig. 18A). Second, while the widths of these areas are uncertain, connection patterns of AI in the present study and of AI and R in previous studies in New World monkeys (FitzPatrick and Imig, '80; Aitkin et al., '88; Luethke et al., '89; Morel and Kaas, '92) suggest that adjoining projection fields are about the width depicted in Figure 18A. Third, while the cortex surrounding AI and R is difficult to subdivide in traditional architectonic preparations, this cortex is not homogeneous in appearance. In particular, the region designated as CM is distinctive in myeloarchitecture (Fig. 6), as well as in the expression of AchE (Figs. 4 and 7).

In regard to the specific fields, the present CM occupies much of the CM as described from Nissl preparations by

Merzenich and Brugge ('73), with the modification that the present AI extends more caudally to include some of the region previously designated as CM (Fig. 18A and B). This CM is similar in location and proportion to CM of owl monkeys as identified by Imig et al. ('77) and adopted by Morel and Kaas ('92). Fields PL and AI also correspond to fields proposed by Imig et al. ('77) for owl monkeys. PL includes most of the lateral field, L, of Merzenich and Brugge ('73), and AL overlaps much of their field b, since we have extended R rostrally to include cortex devoted to high frequency tones. Much of the present RM, corresponding to RM of owl monkeys (Morel and Kaas, '92), overlaps field a of Merzenich and Brugge, ('73). The capping fields C and RT are from owl monkeys (Morel and Kaas, '92), and no specific boundaries are yet proposed for these fields in macaques. Thus, the present proposal incorporates the architectonic and physiological evidence for fields CM, L, b, and a of Merzenich and Brugge ('73) by renaming fields and adjusting boundaries to develop a scheme that is compatible with previous and present evidence for bordering fields in macaques, the present evidence for a caudal extension of AI and a rostral extension of R, and the evidence for these fields in New World monkeys. Nevertheless, there is considerable uncertainty and urgent need for further experimental studies in macaques to evaluate this proposal.

Cortical and thalamic connections of auditory cortex in macaques

The present results indicate that the ipsilateral cortical connections of auditory cortex include AI connections with other parts of AI, R, CM, RM, PL, and probably AL and C. Thus, ipsilateral connections are limited to subdivisions of the surrounding belt. Callosal connections are largely with frequency-matched portions of AI, and with parts of the surrounding belt. Locations in the PL and AL regions connect broadly with AI, R, other subdivisions of the auditory belt, and more lateral parabelt cortex on the superior temporal gyrus and on the upper bank of the superior temporal cortex. Thus, auditory cortex in macaques seems to include three levels of processing: (1) a pair of primary or primary-like areas, AI and R, in the core, (2) a narrow belt of associated areas with less secure auditory driving and responsiveness to tones, and direct inputs from AI or AI and R, and (3) a lateral parabelt region with inputs from PL and AL of the belt. Both AI and the PL region receive inputs from all three subdivisions of the medial geniculate complex, but PL also has more connections with other associated regions of the auditory thalamus, the suprageniculate nucleus and Po. Thus, both AI and PL receive several thalamic inputs, and the belt receives some of the same thalamic inputs as the primary core.

The above anatomical scheme of processing for auditory cortex for macaques has only rather limited support from previous studies in macaque monkeys, in part because there have been rather few studies of auditory cortex in macaques, and in part because of variations and uncertainties in identifying even the primary subdivision of auditory cortex (Fig. 18). Yet, the proposal is completely consistent with the evidence in New World monkeys that AI connects with R, CM, RM, AL, PL, and C, that PL and AL receive inputs from AI and R and project to the parabelt, and that all three subdivisions of the medial geniculate complex project to AI, R, and PL (see Morel and Kaas, '92).

Early degeneration studies of thalamocortical relations in macaques established that the medial geniculate complex projects to cortex in the region of AI on the lower bank of the lateral fissure but uncertainties remained because the cortical lesions were large, and the lesions of course hampered direct architectonic evaluations of the locations of the lesions (e.g., Walker, '37). Results from subsequent studies where lesions or tracers were placed into the auditory thalamus supported the conclusion that MG_V (the principal nucleus) projects to AI or koniocortex (Mesulam and Pandya, '73; Burton and Jones, '76), but injections were few in number, involved more than one nucleus, and produced label both in and around auditory koniocortex. While Burton and Jones ('76) suggested that MG_V projects only to AI, and MG_D projects only to cortex lateral to AI, there was no strong evidence to support this view, and it now conflicts with present results and evidence from studies in New World monkeys (Luethke et al., '89; Morel and Kaas, '92) and cats (see Imig and Morel, '83). More recently, injections of fluorescent dyes in presumptive AI, identified by parvalbumin reactivity, labeled neurons in all three subdivisions of the medial geniculate complex (Hashikawa et al., '91), as did injections in AI in the present study.

There are few earlier studies of the cortical connections of auditory cortex in macaques. In an important more general study (Galaburda and Pandya, '83), an injection in auditory koniocortex (judged to be AI) revealed dense projections to cortex immediately lateral and medial to koniocortex, as well as more distant locations. While the injection may have involved R (see Fig. 18D), these results, if from AI, are consistent with the present evidence that AI has connections with CM and PL. Furthermore, even a slight involvement of PL in an AI injection could label an array of more distant cortical sites (e.g., Fig. 9B). In an earlier study of connections based on degenerating fibers after lesions of cortex (Pandya et al., '69), a lesion limited to auditory koniocortex produced degenerating ipsilateral projections only in regions of immediately adjoining cortex. Results from this case also revealed callosal connections in cortex closely matching the injection site. Thus, as for the present results, callosal connections seem to be concentrated in the matched auditory region.

The organization of the auditory thalamus

In the present study, we recognized the three traditional architectonic subdivisions of the medial geniculate complex (see Jones, '85), although there was some uncertainty about the exact border between MG_V and MG_D in the Nissl and histochemical preparations. Recent preliminary studies on the distribution of parvalbumin and calbindin in the complex (Hashikawa et al., '91) suggest that immunostaining for these calcium binding proteins may help to better define boundaries. Nevertheless, it was clear that all three nuclei were labeled after injections in AI or the PL region. Furthermore, since injections were placed in areas of cortex where recordings identified the best frequencies of neurons, the locations of neurons projecting to populations of neurons of differing best frequencies were determined. The results provide evidence about the tonotopic organization of auditory nuclei in macaque monkeys. The connection patterns suggest that high tones are represented dorsal and rostral to low tones in MG_V. Similar conclusions were obtained from studies of thalamocortical connections in owl monkeys (Morel and Kaas, '92). More significantly, degeneration patterns in cortex after lesions including different parts of MG_V in macaque monkeys led Mesulam and Pandya ('73) to conclude that rostral MG_V projects caudally

in koniocortex, while caudal MG_V projects more rostrally. This would indicate that rostral MG_V represents high tones, a conclusion similar to the present conclusion that dorsorostral MG_V represents high tones. In cats, the organization in MG_V is slightly rotated, with high tones represented medial to low tones (Imig and Morel, '85).

ACKNOWLEDGMENTS

We thank Sherre Florence and Marcie Pospichal for comments in the manuscript. Dr. Christine Baleydier kindly provided brain sections from macaque monkeys processed for radioactive 2-deoxyglucose. Illustrations were drawn by Judith Ives. The research was supported by NIDCD-00922.

LITERATURE CITED

Aitkin, L.M., M. Kudo, and D.R.F. Irvine (1988) Connections of the primary auditory cortex in the common marmoset, *Callithrix jacchus jacchus*. J. Comp. Neurol. *269:*235–248.

Allman, J.M., and J.H. Kaas (1974) The organization of the second visual area (VII) in the owl monkey: A second order transformation of the visual hemifield. Brain Res. *76:*247–265.

Andersen, R.A., P.L. Knight, and M.M. Merzenich (1980) The thalamocortical and corticothalamic connections of AI, AII, and the anterior auditory field (AAF) in the cat: Evidence for two largely segregated systems of connections. J. Comp. Neurol. *194:*663–701.

Bear, M.F., K.M. Carnes, and F.E. Ebner (1985) An investigation of cholinergic circuitry in cat striate cortex using acetylcholinesterase histochemistry. J. Comp. Neurol. *234:*411–430.

Brodmann, K. (1909) Vergleichende Lokalisationslehre der Grosshirnrinde. Leipzig: Barth.

Burton, H., and E.G. Jones (1976) The posterior thalamic region and its cortical projection in New World and Old World monkeys. J. Comp. Neurol. *168:*249–302.

Clarey, J.C., and D.R.F. Irvine (1990) The anterior ectosylvian sulcal auditory field in the cat: II. A horseradish peroxidase study of its thalamic and cortical connections. J. Comp. Neurol. *303:*304–324.

Felleman, D.J., and D.C. Van Essen (1991) Distributed hierarchical processing in primate cerebral cortex. Cerebral Cortex *1:*1–47.

FitzPatrick, K.A., and T.J. Imig (1978) Projections of auditory cortex upon the thalamus and midbrain in the owl monkey. J. Comp. Neurol. *177:*537–556.

FitzPatrick, K.A., and T.J. Imig (1980) Auditory cortico-cortical connections in the owl monkey. J. Comp. Neurol. *192:*589–610.

Galaburda, A.M., and D.N. Pandya (1983) The intrinsic architectonic and connectional organization of the superior temporal region of the rhesus monkey. J. Comp. Neurol. *221:*169–184.

Gallyas, F. (1979) Silver staining of myelin by means of physical development. Neurol. Res. *1:*203–209.

Geneser-Jensen, F.A., and T.W. Blackstad (1971) Distribution of acetylcholinesterase in the hippocampal region of the guinea-pig. 1. Entorhinal area, parasubiculum, and presubiculum. Z. Zeliforsch. Mikr. Anat. *114:*460–481.

Gibson, A.R., D.I. Hansma, J.C. Houk, and F.R. Robinson (1984) A sensitive low artifact TMB procedure for the demonstration of WGA-HRP in the CNS. Brain Res. *298:*235–241.

Hashikawa, T., E. Rausell, M. Molinasi, and E.G. Jones (1991) Parvalbumin- and calbindin-containing neurons in the monkey medial geniculate complex: Differential distribution and cortical layer specific projections. Brain Res. *544:*335–341.

Imig, T.J., and A. Morel (1983) Organization of the thalamocortical auditory system in the cat. Ann. Rev. Neurosci. *6:*95–120.

Imig, T.J., and A. Morel (1985) Tonotopic organization in ventral nucleus of medial geniculate body in the cat. J. Neurophysiol. *53:*309–340.

Imig, T.J., and R.A. Reale (1980) Patterns of cortico-cortical connections related to tonotopic maps in cat auditory cortex. J. Comp. Neurol. *192:*293–332.

Imig, T.J., M.A. Ruggero, L.M. Kitzes, E. Javel, and J.F. Brugge (1977) Organization of auditory cortex in the owl monkey (*Aotus trivirgatus*). J. Comp. Neurol. *171:*111–128.

Jones, E.G. (1985) The Thalamus. New York: Plenum Press.

Juliano, S.L., P.J. Hand, and B.L. Whitsel (1983) Patterns of metabolic activity in cytoarchitectural area SII and surrounding cortical fields of the monkey. J. Neurophysiol. *50:*961–980.

Kaas, J.H. (1987) The organization of neocortex in mammals: Implications for theories of brain function. Ann. Rev. Psychol. *38:*129–151.

Kaas, J.H., and T.P. Pons (1988) The somatosensory system of primates. In H.P. Steklis (ed), Comparative Primate Biology, Vol. 5: Neuroscience. New York: Alan R. Liss, Inc., pp. 421–868.

Luethke, L.E., L.A. Krubitzer, and J.H. Kaas (1988) Cortical connections of electrophysiologically and architectonically defined subdivisions of auditory cortex in squirrels. J. Comp. Neurol. *268:*181–203.

Luethke, L.E., L.A. Krubitzer, and J.H. Kaas (1989) Connections of primary auditory cortex in the New World monkey, Saguinus. J. Comp. Neurol. *285:*487–513.

Merzenich, M.M., and J.F. Brugge (1973) Representation of the cochlear partition on the superior temporal plane of the macaque monkey. Brain Res. *50:*275–296.

Mesulam, M.-M., and E.J. Mufson (1985) The insula of Reil in man and monkey: Architectonics, connectivity, and function. In A. Peters and E.G. Jones (eds): Cerebral Cortex, Vol. 4, Association and Auditory Cortices. New York: Plenum Press, pp. 179–226.

Mesulam, M.M., and D.N. Pandya (1973) The projections of the medial geniculate complex within the sylvian fissure of the rhesus monkey. Brain Res. *60:*315–333.

Mesulam, M.-M., A.D. Rosen, and E.J. Mufson (1984) Regional variations in cortical cholinergic innervation: Chemoarchitectonics of acetylcholinesterase-containing fibers in the macaque brain. Brain Res. *311:*245–258.

Morel, A., and J.H. Kaas (1992) Subdivisions and connections of auditory cortex in owl monkeys. J. Comp. Neurol. *318:*27–63.

Morel, A., P.E. Garraghty, M.K. Schwaber, P. Burch-Sims, and J.H. Kaas (1991) Tonotopic organization, architecture and connections of auditory cortex in macaque monkeys. Soc. Neurosci. Abstr. *17:*305.

Morino-Wannier, P., S.C. Fujita, and E.G. Jones (1992) GABAergic neuronal populations in monkey primary auditory cortex defined by co-localized calcium binding proteins and surface antigens. Exp. Brain Res. *88:*422–432.

Pandya, D.N., and F. Sanides (1973) Architectonic parcellation of the temporal operculum in rhesus monkey and its projection pattern. Z. Anat. Entwickl. Gesch. *139:*127–161.

Pandya, D.N., and E.H. Yeterian (1985) Architecture and connections of cortical association areas. In A. Peters and E.G. Jones (eds): Cerebral Cortex, Vol. 4, Association and Auditory Cortices. New York: Plenum Press, pp. 3–61.

Pandya, D.N., M. Hallett, and S.K. Mukherjee (1969) Intra- and interhemispheric connections of the neocortical auditory system in the rhesus monkey. Brain Res. *14:*49–65.

Robertson, R.T. (1987) A morphogenic role for transiently expressed acetylcholinesterase in developing thalamocortical systems. Neurosci. Lett. *75:*259–264.

Robertson, R.T., F. Mostamand, G.H. Kageyama, K.A. Gallardo, and J. Yu (1991) Primary auditory cortex in the rat: Transient expression of acetylcholinesterase activity in developing geniculocortical projections. Dev. Brain Res. *58:*81–95.

Tootell, R.B.H., S.L. Hamilton, and M.S. Silverman (1985) Topography of cytochrome oxidase activity in owl monkey cortex. J. Neurosci. *5:*2786–2800.

von Bonin, G., and P. Bailey (1947) The Neocortex of *Macaca mulatta*. Urbana: University of Illinois Press.

Walker, A.E. (1937) The projection of the medial geniculate body to the cerebral cortex in the macaque monkey. J. Anat. (London) *17:*319–331.

Wallace, M.N., L.M. Kitzes, and E.G. Jones (1991) Chemoarchitectonic organization of cat primary auditory cortex. Exp. Brain Res. *86:*518–526.

Wong-Riley, M. (1979) Changes in the visual system of monocularly sutured or enucleated cats demonstrable with cytochrome-oxidase histochemistry. Brain Res. *171:*11–28.